

**INTERNATIONAL FUND FOR AGRICULTURAL DEVELOPMENT
(IFAD)**

**FOOD AND AGRICULTURE ORGANIZATION OF THE UNITED
NATIONS (FAO)**

Mexico BALSAS Project

Basin Approaches for Livelihood Sustainability through Adaptation Strategies

**Climate change trends, trajectories and impacts in the BALSAS Project
Area**

Final report

Aldo Daniel Jiménez Ortega (Consultant)

02/10/2022

Content

1. Executive summary	3
2. Introduction	4
Methodology	7
3.1. Climate trends and trajectories	7
3.2. Effects of climate change	10
4. Results	12
4.1. Climate trends and paths	12
4.1.1. <i>El Niño-Southern Oscillation</i>	12
4.1.2. <i>Intermountain depressions</i>	14
4.1.3. <i>South Pacific Coastal Plain and Lomerío Hills</i>	21
4.1.4. <i>Temperate mountain ranges of the Sierra Madre del Sur</i>	27
4.1.5. <i>Temperate mountain ranges of the Transverse Neovolcanic System</i>	34
4.2. Effects of climate change	40
4.2.1. <i>Vulnerability to climate change and hazards</i>	40
4.2.2. <i>Disasters</i>	43
5. Conclusions	50
References	53

Executive summary

In this study, the climate rationale for the BALSAS Project was developed based on the identification of climatological trends and trajectories, as well as the effects of climate change in the project area, which comprises the Balsas Basin and surrounding municipalities. Given the climatic heterogeneity of the area, the identification of climatological trends and trajectories was carried out in a differentiated manner for the four major ecoregions of the project area: intermontane depressions; coastal plains and lomerios of the South Pacific; Sierra Madre del Sur and; the Transversal Neovolcanic System. Climatological data from 262 stations were used for the analysis period 2000-2018 and the reference period 1970-1999. From these data, trends in precipitation, minimum temperature, maximum temperature, anomalies, dry and rainy days, as well as the presence of drought and extreme humidity events were identified. Future trajectories (2041-2060) of precipitation and temperature under trend and pessimistic simulations of greenhouse gas emissions associated with development models were also incorporated. The effects of climate change in the project area were analyzed based on the relationship between the dynamics of the El Niño-Southern Oscillation (ENSO) system with municipal information on vulnerability to climate change, hazards and risks from hydrometeorological phenomena, as well as emergency and disaster declarations for droughts, rains and floods, tropical cyclones and frost, hail and snowfall.

The results showed an increase in temperature patterns, changes in precipitation trends, frequency and intensity of dry/wet events and impacts of extreme events, as evidence of the effects of climate change. An increasing temperature trend was observed in the study area with variations according to each ecoregion. This is highly relevant for an area where most of the rural population's livelihoods depend on agriculture, as any long-term temperature variation has a significant impact on crop production. Furthermore, future simulations accentuate the need for adaptation and mitigation measures, as increases of 2 to 3.6 °C in average annual maximum temperature and 1.76 to 4 °C are projected. Regarding precipitation, the results show an increasing trend that became more pronounced from 2010 onwards and, with it, larger positive anomalies and more humid days with more intense rainfall. This pattern was accompanied by the transition from a period (1970-1999) where the dry phase predominated to a period where the wet phase predominated (2000-2018). Finally, it was observed that hazards and risks due to hydrometeorological phenomena show differences by ecoregion, while emergency and disaster declarations were associated with the ENSO dynamics.

2. Introduction

Climate change is a dynamic process of changing temperatures and patterns of atmospheric conditions over the long term, which affects the environment and people around the world (Kellstedt et al., 2008). Anthropogenic activities are the main drivers of climate change. Examples of these activities are the burning of fossil fuels and deforestation, which have increased CO₂ levels in the atmosphere (Huckelba & Van Lange, 2020). This has led to a reconfiguration of the system, expressed in the acceleration of global warming, intensification of the water cycle, melting of glaciers and permafrost, rising sea levels, ocean acidification and warming, intensification of climate variability and climate extremes associated with El Niño-Southern Oscillation, among others (Nunes & Ferreira, 2022; Yun et al., 2021; IPCC, n.d.). This is all the more relevant considering that current global emissions trends are heading towards the most pessimistic future scenario (8.5 RCP or SSP585) (Moore et al., 2021).

A number of indicators have been developed to generate evidence of climate change impacts at different spatial scales. Among the most common are monthly and annual temperature averages, seasonal temperature averages, trends in hot and dry days, precipitation anomalies, frequency of high intensity rainfall events (days), tropical cyclone activity, droughts, among others (Khan et al., 2022; Cubasch et al., 2013; EPA, n.d.). Another aspect to identify the effects of climate change on populations and the environment are climate disasters, which occur when extreme weather events interact with vulnerable social, economic and environmental conditions (Valera, 2019).

In the Balsas Basin, located in south-central Mexico, different socio-ecological landscapes, both rural and urban, converge. It is a heterogeneous hydrological region in its biophysical and socio-economic components, with high water vulnerability and strong erosion processes, which are the result of the interaction between steep slopes, intense rainfall and deforestation processes that disrupt the regulation of the hydrological cycle and generate a series of dangers for the livelihoods of the population, which presents high levels of marginalisation and social backwardness in most of the municipalities (Melgarejo et al., 2021; Valencia-Vargas, 2015).

In the context of this problem, in mid-2020, the Mexican government asked the International Fund for Agricultural Development (IFAD) to develop an investment project proposal that could also be co-financed by the Green Climate Fund (GCF). This project called "BALSAS: Basin Approaches for Livelihood Sustainability through Adaptation Strategies" aims to reduce the vulnerability to climate change of the rural population, ecosystems and production systems and to enhance the transformation towards sustainable, more resilient and low-emission agricultural and forestry production models in the BALSAS Project Area (BPA), which comprises the Balsas Basin and its surroundings. A

mandatory requirement to be included in the formulation of funding proposals is climate rationality. Climate rationale is the scientific evidence-based justification that the GCF has requested from developing countries and accredited entities to support project proposals (Valera, 2019). According to the GCF, "*climate rationale is established by providing an evidence-based analysis to show that a proposed activity is likely to be an effective adaptation response to the risk or impact of a specific climate change hazard*". The four principles that the GCF sets out to drive the climate rationale for adaptation proposals are as follows:

- a) Identification: Adaptation proposals should show how the activity addresses the risk or impact of current or projected future climate change, and why it is likely to be an effective response. Proposals should identify the systems at risk and the climate change hazard that affects them or is expected to do so in the future. They should show how climate change has led, or will lead, to the specific risk or impact addressed by the proposed activity using the best available information. Where appropriate, proposals should also consider any non-climate factors that may be causing or exacerbating the risk or impact and describe the interactions between climate change and non-climate factors. Vulnerability assessments can be used to identify groups, sectors and sub-regions most susceptible to the impact of climate change and will therefore provide information for selecting and prioritising appropriate adaptation outcomes.
- b) Response: Proposals should explain how the activity will reduce exposure and/or vulnerability (of people, systems or ecosystems) and thereby reduce the risk or impact of climate change. Where appropriate, a justification should be provided as to why the proposed activity was selected over alternatives. Proposals should consider the barriers (e.g. technical, social, institutional, regulatory) to the implementation of the activity and describe how the project intends to overcome these barriers. Proposals should apply a methodological approach to the quantification of the number of beneficiaries expected to result from the activity.
- c) Alignment: Proposals should confirm the alignment of the proposed activity with the host country's national plans and climate strategies. This helps to ensure that the country has ownership of the proposal and that activities are targeted to the areas of greatest potential need and impact for that country.
- d) Monitoring and evaluation: Projects with a well-designed theory of change are more likely to generate successful outcomes that can be measured and evaluated. Proposals should include a description of the monitoring and evaluation system that will be used to assess the climate impact¹ of the proposed activity and quantify the beneficiaries of adaptation. This

will facilitate assessment during implementation of whether the funded activity generated the expected climate impact and will also inform the design of future, more impactful adaptation options.

The objective of this study is to generate climate rationality for the BALSAS Project by identifying the trends and impacts of climate change in the BPA, with the aim of justifying the intervention based on adaptation measures in territories with priority populations in a situation of marginalisation and vulnerability. The results of the study are shown in two sections: 1) Climate trends and trajectories; and 2) Climate change effects.

3. Methodology

The methodology is structured in two main sections: 1) climatological trends and trajectories and, 2) effects of climate change. The first section describes the data and procedures for the identification of El Niño-Southern Oscillation (ENSO) dynamics, trends and trajectories of precipitation, temperature, anomalies, dry and rainy days, drought and wet events, as well as future trends. The second section describes the resources used to identify the vulnerability of the basin to climate change and the hydrometeorological hazard risks to which it is exposed.

3.1. Climate trends and trajectories

The unit of analysis for the identification of climatological trends and trajectories was the ecoregion. Terrestrial ecoregions make it possible to establish zones with relative climatic and ecosystemic homogeneity, thus allowing for differentiated analyses based on the averages of climatological information from the stations. For this purpose, vector data of terrestrial ecoregions at a scale of 1:1,000,000 (INEGI-CONABIO-INE, 2007) were used, resulting in four large terrestrial ecoregions and one with a small surface area (Figure 1), which was not included in the analysis due to insufficient climatological information. The ecoregions integrated in the analysis are: 1) Intermontane depressions with low deciduous forest and xerophytic scrub (DI); 2) Coastal plain and lomerios of the South Pacific (PCP); 3) Temperate mountain ranges of the Sierra Madre del Sur (SMS) and; 4) Temperate mountain ranges of the Transverse Neovolcanic System (TNS). The results of this section were presented separately for each ecoregion.

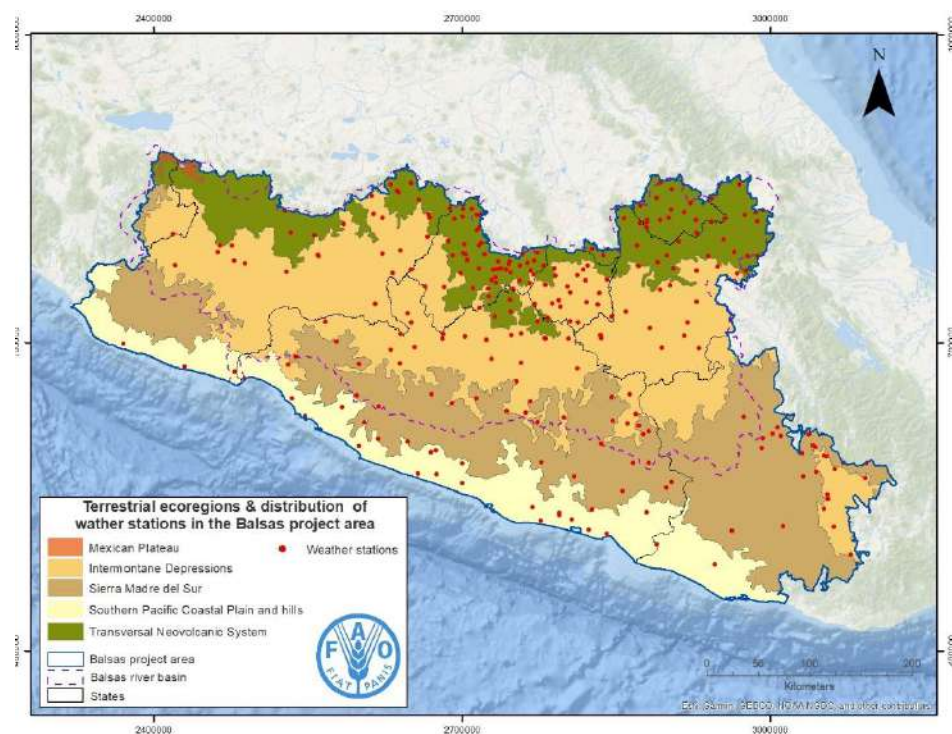


Figure 1. Map of terrestrial ecoregions of the BALSAS project area

Daily climatological data from the stations located in the BPA were obtained from the Hydrological Information System (SIH) of the National Water Commission (CONAGUA, sf). Data from 1,251 stations were reviewed, of which 262 were selected (Annex 1) distributed in the four ecoregions (Table 1). This selection was based on the criterion of highest monthly data availability for both periods, so those stations that did not have sufficient data were discarded. From the review it was observed that 2018 was the last year with sufficient data at the stations that had data since 1970, so the study period was defined as 2000-2018 and the reference period as 1970-1999.

Table 1. Distribution of weather stations by terrestrial ecoregions

Terrestrial ecoregion	Weather stations	Balsas Project area
Intermontane depressions	106	39%
Southern Pacific coastal plain and hills		14%
Sierra Madre del Sur		31%
Transversal neovolcanic system	92	16%

The averages of the climatological variables of the stations in each ecoregion were obtained and the trends in the study period and differences in relation to the average observed in the reference period were observed. The following variables were obtained from the climatological data: average monthly precipitation, average annual precipitation, average monthly maximum temperature, average annual maximum temperature, average monthly minimum temperature, average annual minimum

temperature. The variables used in this study were selected due to three main reasons: 1) they are considered essential to understand the evolution of surface climate when seeking to establish adaptation and mitigation measures to climate change (Bojinski et al., 2014); 2) their changes can increase the probability of occurrence of extreme events (Moustakis et al., 2020) and; 3) changes in precipitation and temperature affect the quantity and yield of crops (Jia et al., 2022).

The calculation of the anomalies of precipitation, maximum temperature and minimum temperature was made by the difference between the observed value of each month and the monthly historical average of the variable for the period 1970-2018. With these calculations, the monthly variation in terms of millimetres or °C per month was observed. Likewise, the calculation of dry days and rainy days was carried out, considering the former as those with precipitation less than 1 mm and the latter as those with precipitation greater than or equal to 1 mm. The intensity of rainy days was obtained from the rainfall intensity classification (Table 2) of Qian et al. (2014). Trend analysis of these indicators was performed by differentiating the rainy season (June-October) and the dry season (January-May and November-December).

Table 2. Classification of rainfall intensity (Quian et al., 2014)

Grade	Rainfall amount of 24 h (mm)
Small rain	< 10
Moderate rainfall	10 - 25
Heavy rainfall	25 - 50
Storm	50 - 100
Large storm	100 -250
Extreme large storm	≥ 250

Droughts and wet events were identified using the Standardised Precipitation-Evapotranspiration Index (SPEI), which incorporates precipitation and potential evapotranspiration values, allowing the results to be associated with the effects of climate change (Vicente-Serrano et al., 2010). Potential evapotranspiration (PTE) was obtained from the Hargreaves (1985) equations, based on temperature and radiation defined by the latitude of the station/ecoregion centroid.

$$ETP = 0.0023(T_{media} + 17.8)(T_{max} - T_{min})^{0.5} Ra$$

From the ETP, the climate balance was obtained by calculating the difference between precipitation and ETP. The results were standardised using a log-logistic function at a 12-month scale (Vicente-Serrano et al., 2010). The SPEI calculation was performed using the SPEI version 1.7 package in RStudio software.

Table 3. The Standardize Precipitation-Evapotranspiration Index (Vicente-Serrano et al., 2010)

SPEI	Drought/wet severity
≤ 2	Extreme drought
-1.99 - -1.50	Severe drought
-1.49 - -1.00	Moderate drought
-0.99 - 0.99	Near normal
1.00 - 1.49	Moderately wet
1.50 - 1.99	Severely wet
≥ 2	Extremely wet

The analysis of future climate trajectories was performed using the HadGEM3 simulation, which is part of the sixth Coupled Model Intercomparison Project contribution, CMIP6 (Andrews et al., 2020). This simulation was selected because its spatial resolution is compatible at the ecoregion level. For this purpose, raster data of the climatological variables total monthly precipitation, average monthly maximum temperature and average monthly minimum temperature were used, which were obtained from WorldClim (Sf) at a spatial resolution of 30 seconds for the period 2041-2060. The data used correspond to two socio-economic trajectories (SSPs), which are narratives that drive the models as a function of greenhouse gas emissions under different development guidelines (Riahi et al., 2017). The two socio-economic trajectories used correspond to a baseline development model in the absence of climate policies (SSP245) and a fossil-fuel intensive one (SSP858). The raster data were cropped for the BPA ecoregions and the differences of the three variables with respect to the averages for the period 2000-2018 were calculated.

3.2. Effects of climate change

The vulnerability of the ABS to climate change, as well as hydrometeorological risks and hazards, were addressed using data from the National Institute of Ecology and Climate Change (INECC, 2019) and the National Centre for Disaster Prevention (CENAPRED), with the municipality being the unit of analysis for these results. The climate change vulnerability data show three categories of vulnerability: first level, second level and third level. These levels are based on six specific vulnerabilities: 1) vulnerability of human settlements to landslides; 2) vulnerability to floods; 3) vulnerability to the potential increase of vector-borne diseases (dengue); 4) vulnerability of livestock production to water stress; 5) vulnerability of livestock production to floods and; 6) vulnerability of forage production to water stress. In addition, the vulnerability levels used in this study include future vulnerability based on projections from four general circulation models. According to INECC (2019) the models used are Centre National de Recherches Météorologiques (CNRMCM5), Geophysical Fluid Dynamics Laboratory (GFDL-CM3), Met Office Hadley Center (HADGEM2-ES) and Max

Plank Institute for Meteorology (MPI-ESM-LR), for the time horizon 2015-2039 and for the Representative Concentration Path (RCP) 8.5. W/m².

For risks and hazards due to hydrometeorological phenomena, vector data were used for the different degrees of danger due to droughts, floods, tropical cyclones and frost. Drought hazard degree data were obtained from CENAPRED (2012). These vector data correspond to a classification of the index proposed by Escalante Sandoval et al (2005), which integrates the average rainfall deficit with respect to the average annual rainfall, as well as the duration of the average drought. The flood risk data show the categories derived from the floodability index proposed by the National Water Commission (CONAGUA, 2016) based on topographic, climatological, land use and soil type variables considering a return period of five years (Montealegre Zúñiga & Matías Ramírez, 2021). The construction of this layer also involved the population that is most vulnerable to being affected by flooding. The data on the degree of risk from tropical cyclones correspond to categories derived from the tropical cyclone hazard index, which integrates the trajectories and intensity of these phenomena since 1940 (Jiménez Espinosa et al., 2012), as well as the social vulnerability index. The frost hazard data show the frost index categories of days with frost from the isolines obtained based on Vidal & García (2007).

Finally, disasters derived from the effects of climate change on populations were addressed on the basis of the municipal declarations¹ of emergency or disasters due to drought, rainfall and flooding, tropical cyclones, hail, snowfall and frost. The declarations were obtained for the study period with data from CENAPRED (sf). Patterns in the frequency of declarations were analysed in conjunction with ENSO dynamics.

¹ According to the Ministry of Security and Citizen Protection (DOF, 2021a), a declaration of emergency is the "act by which the Ministry of Security and Citizen Protection, through the CNPC, recognises that one or several municipalities or territorial districts of one or more federal entities are facing the imminence, high probability or presence of an abnormal situation generated by a natural hazard, and therefore immediate assistance is required to the population whose safety and integrity are at risk". On the other hand, a disaster declaration is "the act by which the Ministry of Security and Citizen Protection, through the CNPC, recognises the presence of a Natural Disaster Phenomenon in certain municipalities or municipalities of a Federal Entity, which, according to what has been stated by the Federal Entity, the damage exceeds the local financial and operational capacity for its attention" (DOF, 2021b).

4. Results

4.1. Climate trends and trajectories

4.1.1. El Niño-Southern Oscillation

El Niño-Southern Oscillation (ENSO) is an oceanic-atmospheric system in the tropical Pacific modulating global climate and the dominant mode of interannual variability in the tropics (Pinherio et al., 2022). ENSO results from atmospheric and oceanic changes in high pressure centres from the western equatorial Pacific to the eastern equatorial Pacific (Feingold, 2011). This system is one of the main global drivers of atmospheric climate variability that can persist for several seasons, generating severe regional effects (Zhang et al., 2019; NOAA^a, n.d.). The ENSO system has three phases: a neutral phase and two extreme phases called El Niño (warm phase) and La Niña (cold phase). In Mexico, El Niño has effects associated with stronger and longer dry periods, while La Niña amplifies rainfall (Poveda and Mesa, 1996). There are indications that climate change affects ENSO dynamics through increased atmospheric CO₂, which causes a weakening of future ENSO sea surface temperature variability (Wengel, 2021). This variability may increase the frequency and intensity of extreme events, which can lead to hazardous weather conditions with potential impacts on the livelihoods of rural populations, particularly agriculture (Blanco-Macías et al., 2020).

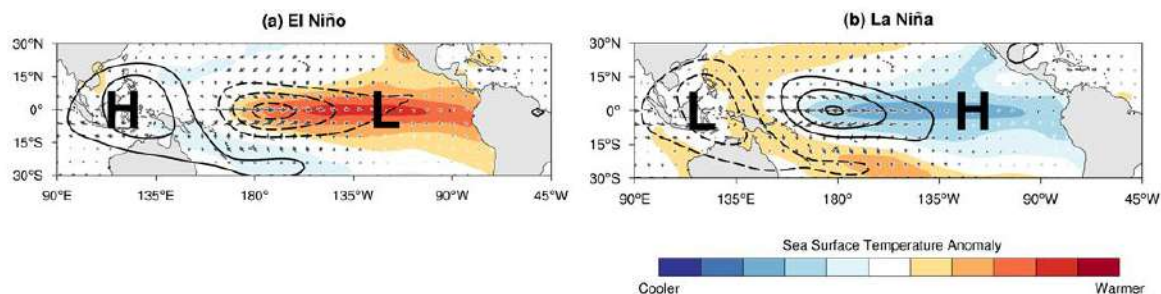


Figure 2. Schematic diagram showing the physical mechanisms by which the SST (shaded), OLR (contours), surface zonal and meridional winds (vectors), and sea level pressure (represented by "H" and "L" which indicate the high and low pressure centre, respectively) determine the wintertime Multivariate ENSO Index (MEI) during (a) El Niño and (b) La Niña events.

Source: NOAA-Physical Sciences Laboratory

Based on NOAA data, MEIv2 values for the period 2000-2018 show a higher frequency of neutral years and La Niña events, as well as higher severity in El Niño years. The years 2004-2005, 2006-2007 and 2014-2015 were classified as weak El Niño; 2002-2003 and 2009-2010 were moderate El Niño, while 2015-2016 was classified as very strong (NOAA^b, n.d.). The latter event, also considered a canonical El Niño, showed different characteristics from previous El Niño events because the Eastern Pacific Intertropical Convergence Zone did not cross southern Ecuador (Malgarejo et al.,

2021). Due to this condition, it has been documented that, despite its intensity, this event did not have the impact on prolonged and intense droughts within the ABS, unlike other El Niño years, such as 2005, which presented anomalies in sea surface temperature and an extensive record in tropical storms and hurricanes (Trenberth et al., 2006; Malgarejo et al., 2021). In the case of La Niña, weak intensities are observed in 2000-2001, 2005-2006, 2008-2009, 2016-2017 and 2017-2018; moderate intensities in 2011-2012; and strong intensities in 2007-2008 and 2010-2011. Increased precipitation levels during the summer and droughts during the winter have been documented (Magaña et al., 2003). These patterns have been observed in the mountainous areas of the Purepecha Plateau, in the Neovolcanic Transversal System of the BPA, in the work of Pinilla Herrera and Pinzón Correa (2016).

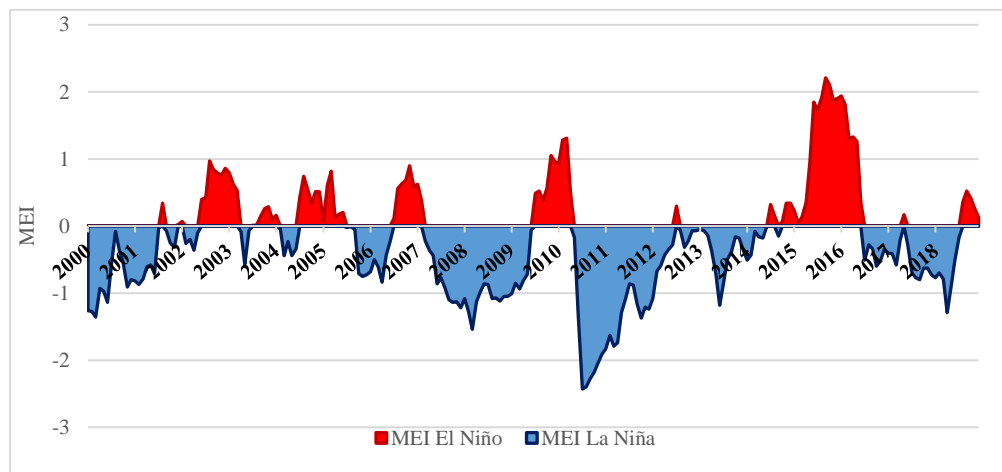


Figure 3. Multivariate ENSO Index 2000-2018 (NOAA, sf)

4.1.2. Intermountain depressions

Temperature and precipitation

Precipitation in the DI has had an increasing trend between 2000 and 2018. The average recorded during this period was 909 mm per year, while in 2010, 2014 and 2017 annual precipitation values were above 1000 mm. During much of this period, precipitation levels have been higher than the average recorded between 1970 and 1999, which was 865 mm per year. The years 2000 and 2005 recorded significantly lower precipitation values than those observed during the study period. The increase in precipitation is mainly observed during the months of May, August and September, with the latter showing the greatest difference.

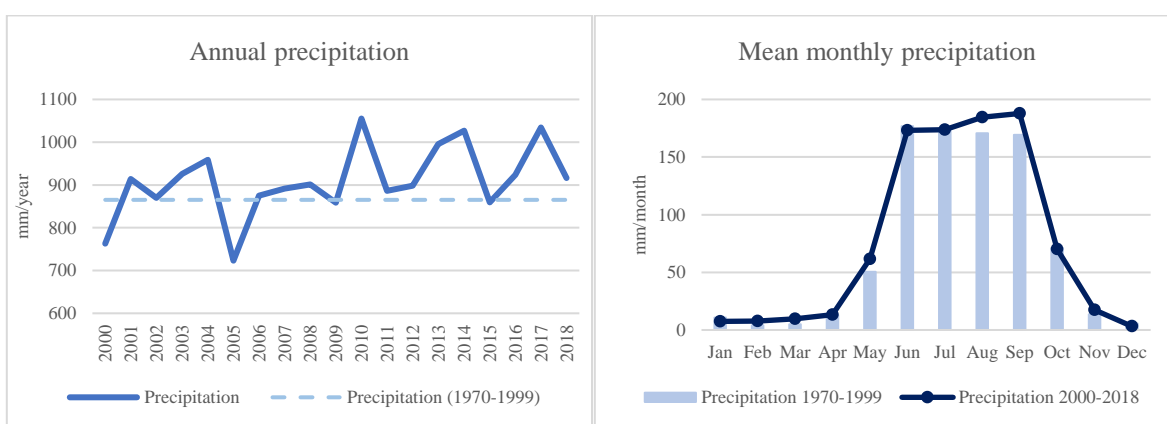


Figure 4. Annual precipitation & mean monthly precipitation in ID

In terms of temperature, records show an increasing trend between 2000 and 2018. This trend was mainly driven by increases in the maximum temperature, which recorded an annual average value of 31.2°C. During much of this period, the average annual maximum temperature was higher than the average value recorded between 1970-1999, especially from 2005 onwards. The months with the largest increases in maximum temperature between the two periods were July (0.53°C), August (0.43°C) and May (0.36°C). Minimum temperature also showed an increasing trend between 2000 and 2018, although during most of this period values were below the annual average for the period 1970-1999. The main variations in minimum temperature in both periods were observed in June and July, with decreases of 0.37°C and 0.23°C, respectively.

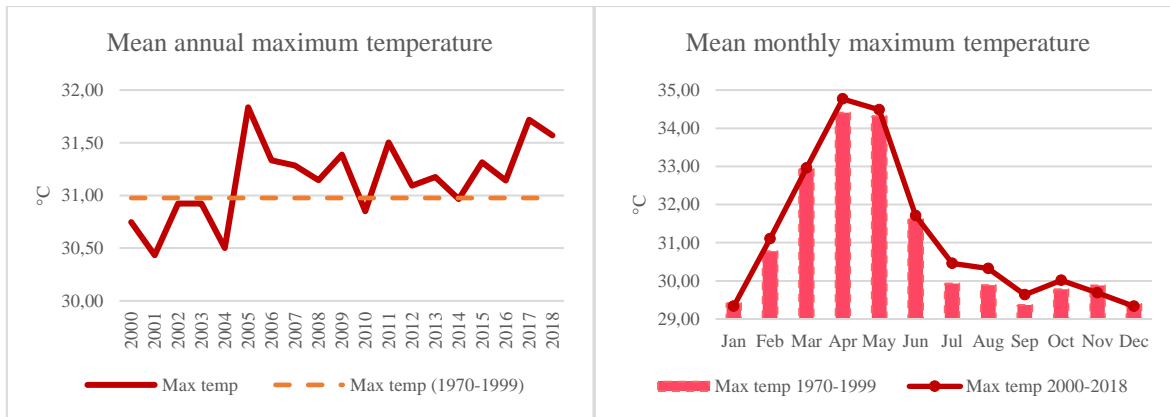


Figure 5. Mean annual maximum temperature & mean monthly maximum temperature in ID

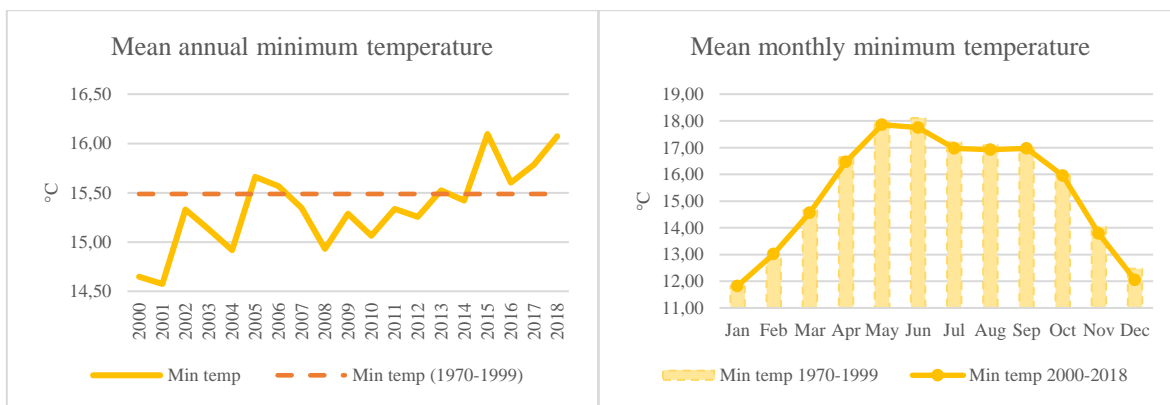


Figure 6. Mean annual minimum temperature & mean monthly minimum temperature in ID

Anomalies

Precipitation anomalies have changed their behaviour between the study period and the reference period. On the one hand, between 1970 and 1999, it was observed that most of the monthly anomalies presented negative values. During this period, 4.2% of the months had rainfall 50 mm or less than average, while 3.6% had rainfall 50 mm or more above average. Between 2000 and 2018, monthly anomalies with positive values were predominant. It was observed that 7.5% of the months exceeded the average monthly values by 50 mm or more, while only 3.1% reported values below average values by 50 mm or less.

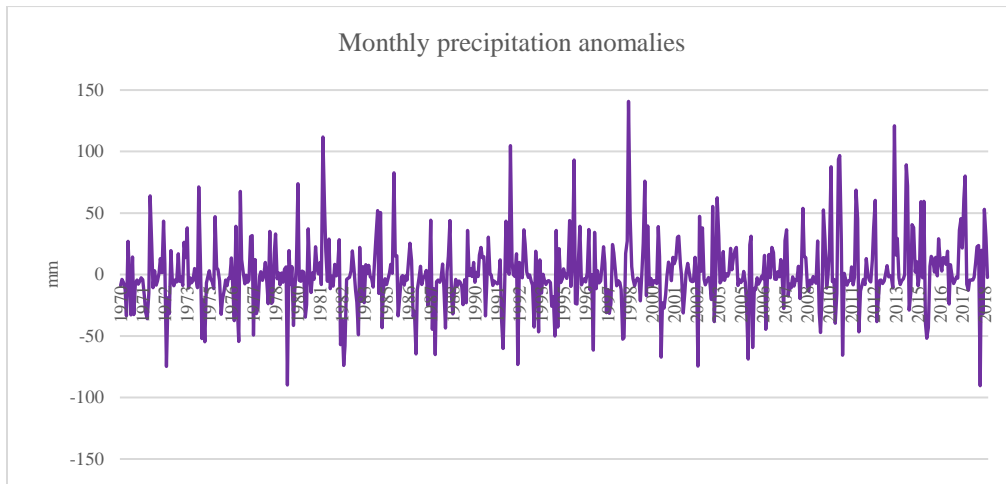


Figure 7. Monthly precipitation anomalies in ID

In terms of temperature, a trend towards a greater number of positive anomalies was observed. On the one hand, in the maximum temperature, 10.6% of the months in the period 1970-1999 showed values 1°C or less below the average value, while 8.6% recorded values 1°C or more above the average. Between 2000 and 2018, 7.9% of the months recorded values lower by 1°C or less than the average maximum temperature, while 9.2% showed values higher by 1°C or more than the reported average. In the minimum temperature, between 1970 and 1999, 22 months recorded temperatures 1°C or less below the average, while 17 months showed temperatures 1°C or more above the average value. For the period 2000-2018, 22 months recorded temperatures 1°C or less below the average, while 9 months showed temperatures above the average value by 1°C or more.

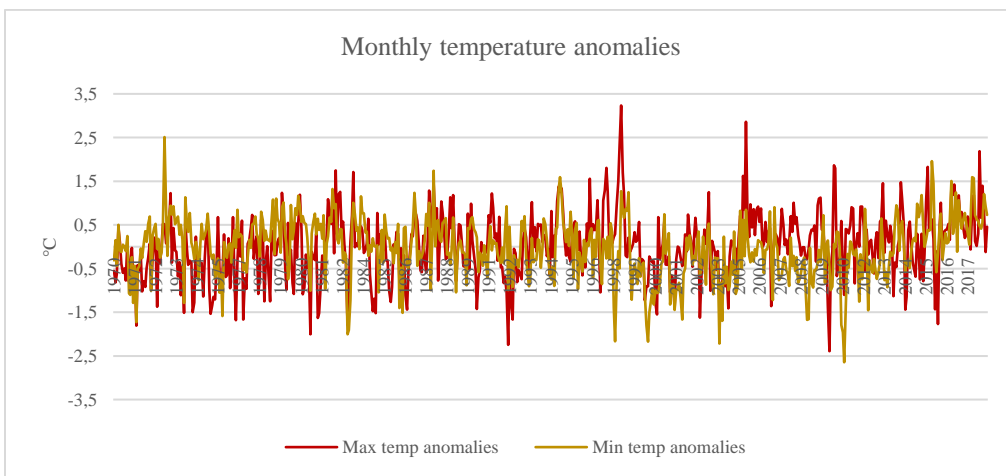


Figure 8. Monthly temperature anomalies in ID

Dry and rainy days

A reduction in the average number of dry days was observed between the periods 1970-1999 and 2000-2018, from 25 to 23 days in the wet season and 186 to 183 in the dry season, respectively. Although these differences are not large in magnitude, changes in dry day trends were identified between the two periods. On the one hand, dry days in the rainy season in the period 1970-1999 showed a decreasing trend, while in the dry season they remained around the average, with more abrupt fluctuations between 1992 and 1998. On the other hand, the number of dry days per year between 2000 and 2018 changed their trends with respect to the previous period, with a decreasing trend in the dry season and a slightly increasing trend in the rainy season.

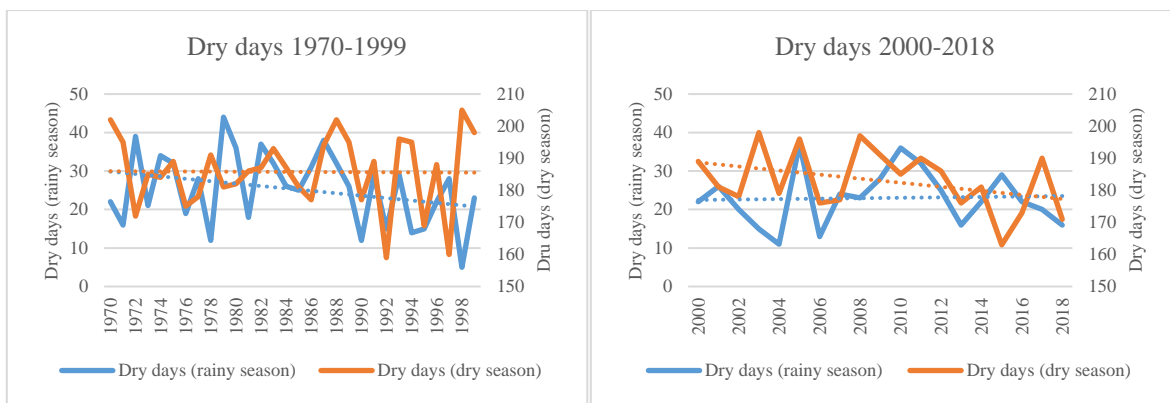


Figure 9. Dry days in ID

The number of rainy days in the DI increased. Between 1970 and 1999, the average number of rainy days per year was 132 in the rainy season and 45 in the dry season, while for the study period it was 140 and 53 rainy days, respectively. In terms of intensity, during the rainy season of the study period, light and moderate rainfall accounted for 90% and 10%, respectively. In the dry season, light and moderate rainfall accounted for 97% and 2.9%, respectively, while the remaining 0.1% corresponds to a heavy rainfall event in 2010. In contrast to the rest of the ecoregions, the intensity of rainy days between 2000 and 2018 decreased compared to the period 1970-1999. In the wet season, light rainfall increased by 1%, while moderate rainfall decreased by 1%. In the dry season, light rainfall increased by 0.6% and moderate rainfall decreased by 0.6%.

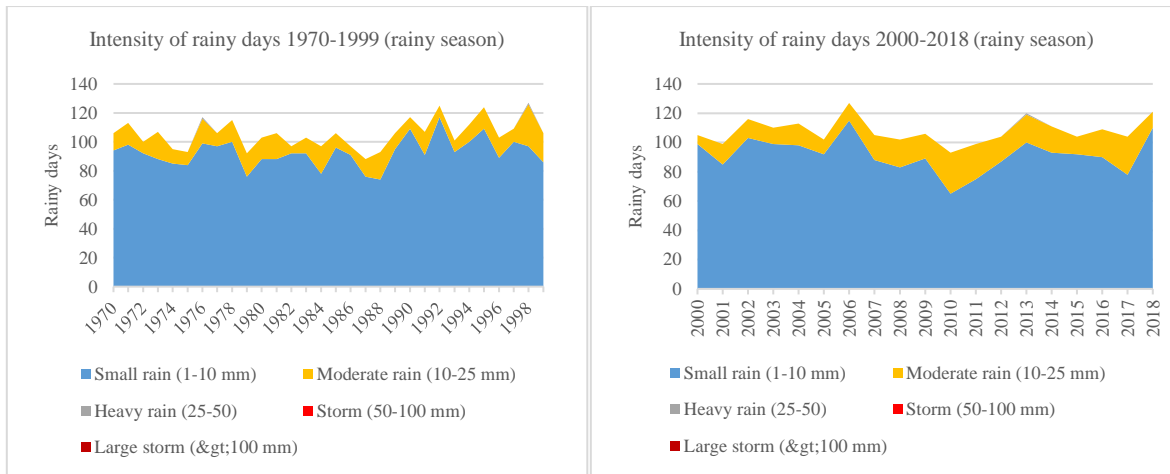


Figure 10. Intensity of rainy days in ID (rainy season)

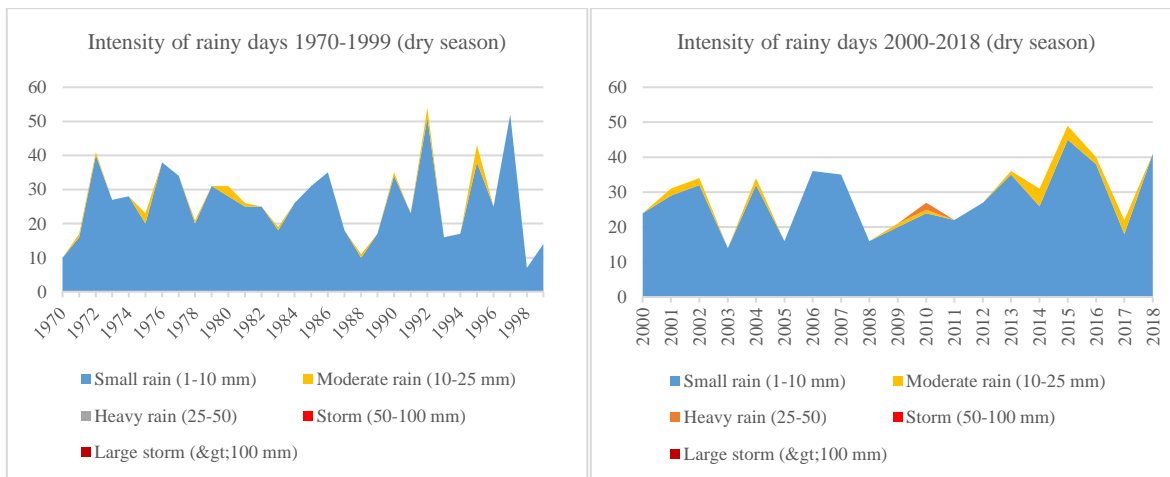


Figure 11. Intensity of rainy days in ID (dry season)

Droughts and wet events

In the DI, a transition from droughts to wet events is observed between the periods 1970-1999 and 2000-2018. According to SPEI data, between 1970 and 2018, 75 drought events were identified (2.5 per year), of which 69% were moderate, 15% severe and 16% extreme. Likewise, 41 wet events (1.4 per year) were recorded, of which 63% were moderate, 15% very wet and 22% extremely wet. During the period 2000-2018, 22 drought events were observed (1.2 per year), of which 59% were moderate, 18% severe and 23% extreme. The years with the most intense and prolonged droughts were 2005 and 2006. On the other hand, 46 wet events were recorded (2.4 per year), of which 52% were moderate, 39% very wet and 9% extremely wet. The years with the most intense wet events were 2014, 2015, 2017 and 2018.

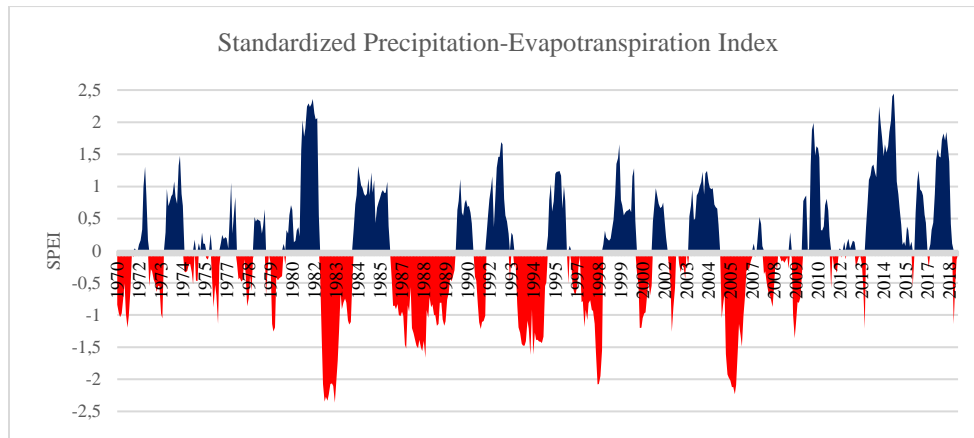


Figure 12. ID-SPEI

Future climate trajectories

The climate trajectories showed a marginal increase by 1.5 mm in average annual precipitation for the period 2041-2060 under SSP245, with respect to the average value for the period 2000-2018. Although this increase is not large, the main changes between the two periods are observed on a monthly basis. In that sense, the main projected increases in precipitation during the rainy season are expected in the months of June and October, with 38 mm and 30 mm respectively, while decreases in precipitation of 37 mm and 14 mm are expected for August and September, respectively. During the dry season, the greatest variation is observed in the months of March and May, with expected reductions of 6 mm and 15 mm, respectively. On the other hand, projections under SSP585 show a reduction in annual precipitation of 43 mm for the period 2041-2060 with respect to the average value for the study period. In the rainy season, the main increase in precipitation was observed in the month of October, with 32 mm, while reductions were recorded in August and September, with 34 mm and 18 mm less than the study period, respectively. In the dry season, the largest variation was recorded in the month of May, with a reduction of 20 mm compared to 2000-2018.

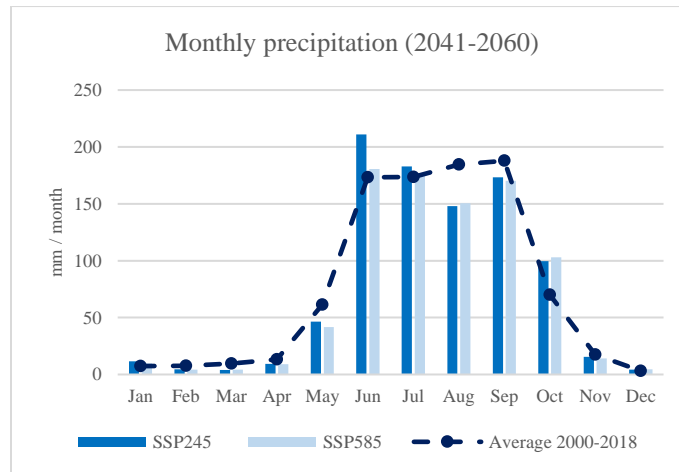


Figure 13. Monthly precipitation in ID (2041-2060)

The largest changes in future trajectories are observed for temperature. The maximum temperature projections for the period 2041-2060 under SSP245 show an increase in annual temperature of 3.05°C over the period 2000-2018. Monthly increases range between 2.5°C and 3.7°C, with June, July, October, November and December showing the largest increases. On the other hand, the maximum temperature simulations for the period 2041-2060 under SSP585 show an increase in annual temperature of 3.6°C. Monthly increases were in the range of 3°C and 4.2°C, with October, November and December showing the largest increases.

Projections of minimum temperature under SSP245 show an increase in annual temperature of 3.18°C over the period 2000-2018. Monthly increases range between 2.4°C and 3.9°C, with January, February and December showing the largest increases. On the other hand, the minimum temperature projections for the period under SSP585 show an increase in annual temperature of 4°C. Monthly increases ranged between 3.07°C and 4.9°C, with the dry season months of January, February, March, May, November and December showing the largest increases.

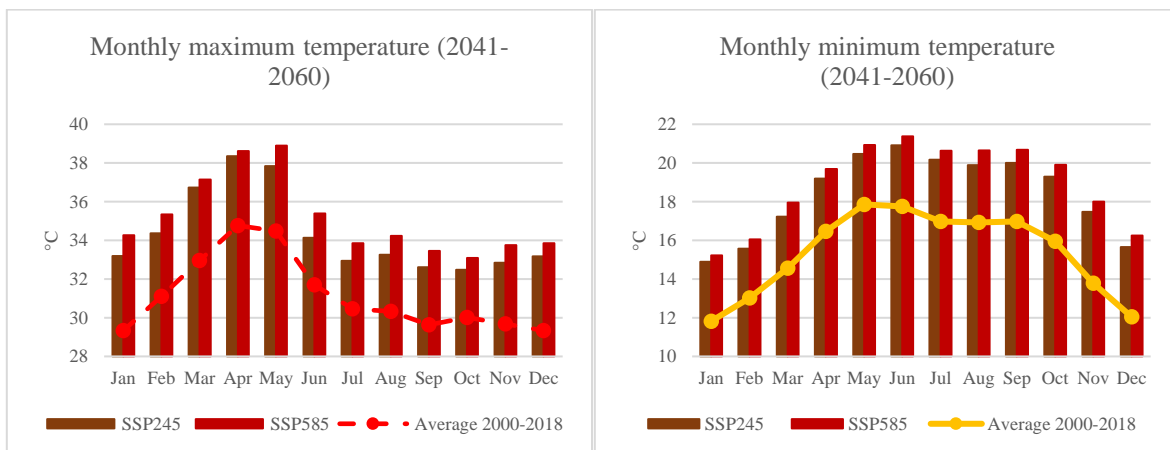


Figure 14. Monthly maximum and minimum temperature in ID (2041-2060)

4.1.3. South Pacific Coastal Plain and Lomerío Hills

In this ecoregion there is no clear trend in annual precipitation averages between periods, nor between 2000 and 2018. However, a greater variation in annual precipitation is observed from 2010 onwards compared to that observed in the first decade of this century. The most relevant changes in average monthly precipitation with respect to 1970-1999 were observed in the months of July, September and October. July recorded on average 24.6 mm less than 1970-1999, while in September and October precipitation was 21.9 mm and 24.5 mm higher, respectively.

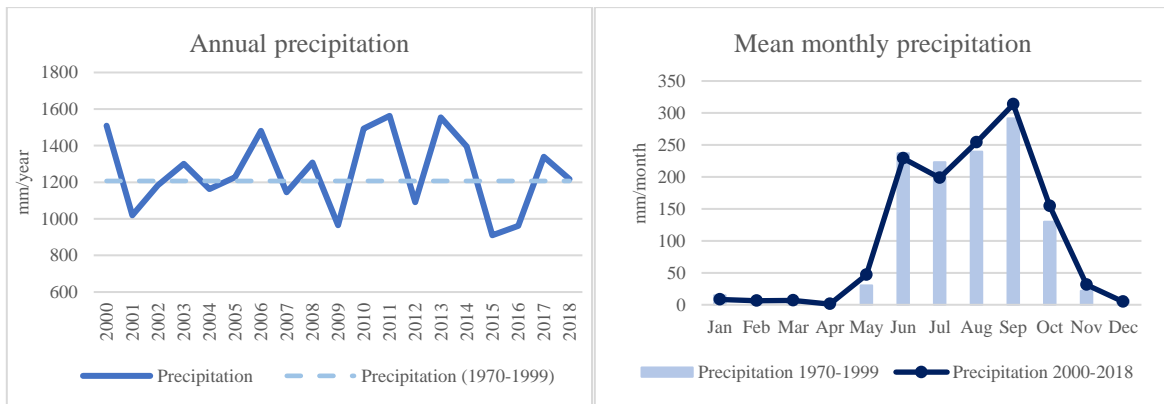


Figure 15. Annual precipitation & mean monthly precipitation in PCP

On the other hand, the temperature in the PCP showed an increasing trend. The average annual maximum temperature did not show a clear trend between 2000 and 2018, however, except for the years 2010 and 2013, the values recorded were higher than the annual average for the period 1970-1999. On average, the annual maximum temperature for the period 2000-2018 was 0.4°C higher than that recorded in 1970-1999, which was 32.1°C. The average monthly maximum temperature of the study period was higher than that of 1970-1999, except for the month of December. The largest increase between the two periods was observed in the months of June to September, with increases between 0.7°C and 0.9°C. On the other hand, an increasing trend was observed in the average minimum temperature during the study period. As in the case of the maximum temperature, the minimum temperature values for most years between 2000 and 2018 were higher than the average for the period 1970-1999. In that sense, the average minimum temperature increased from 20.1°C in 1970-1999 to 20.6°C in 2000-2018. The average monthly minimum temperature was higher than that recorded in 1970-1999. The largest variations were observed in the dry season, particularly in January and February, where the average minimum temperature increased by 1.1°C and 0.9°C, respectively.

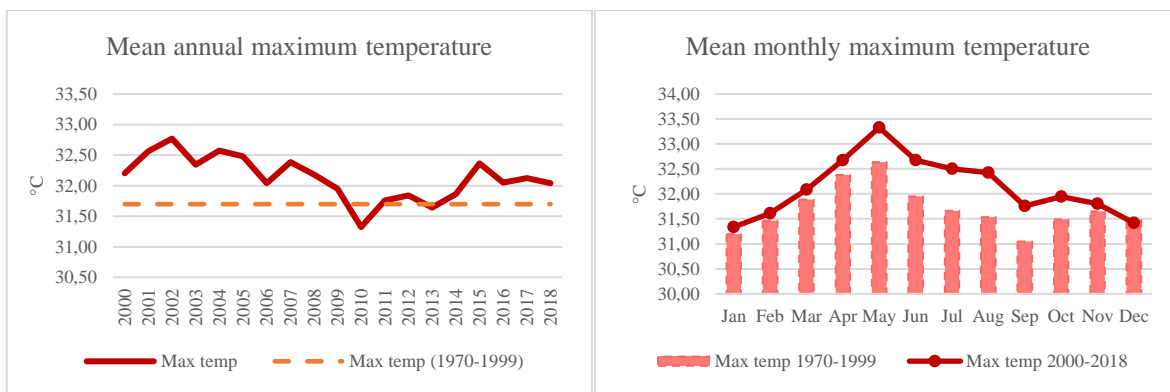


Figure 16. Mean annual maximum temperature & mean monthly maximum temperature in CPH

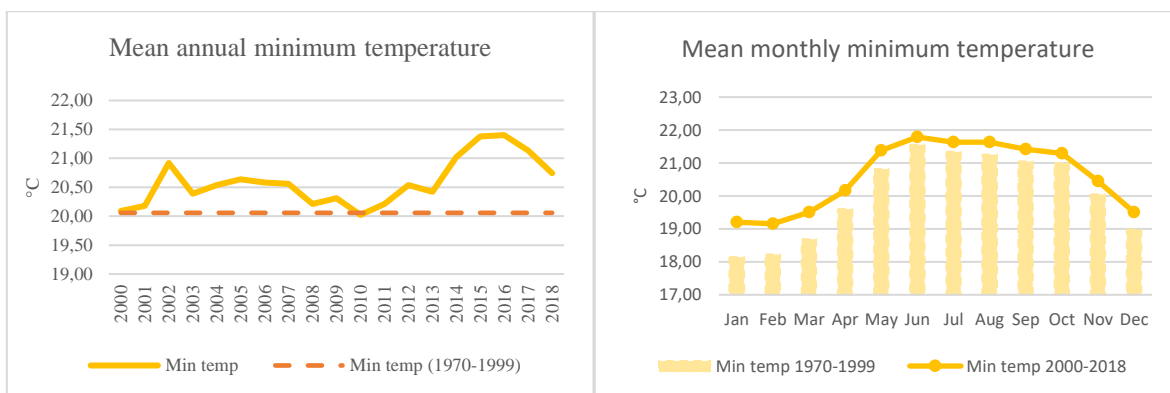


Figure 17. Mean annual minimum temperature & mean monthly minimum temperature in CPH

Anomalies

A change in the behaviour of precipitation anomalies was observed between the two periods. Between 1970 and 1999, most of the monthly anomalies had negative values. During this period, 15% of the months had rainfall 50 mm or less than average, while 11.4% had rainfall 50 mm or more above average. Between 2000 and 2018, the monthly anomalies with positive and negative values were similar. It was observed that 12.7% of the months exceeded the average monthly values by 50 mm or more, while 12.3% reported values below average values by 50 mm or less.

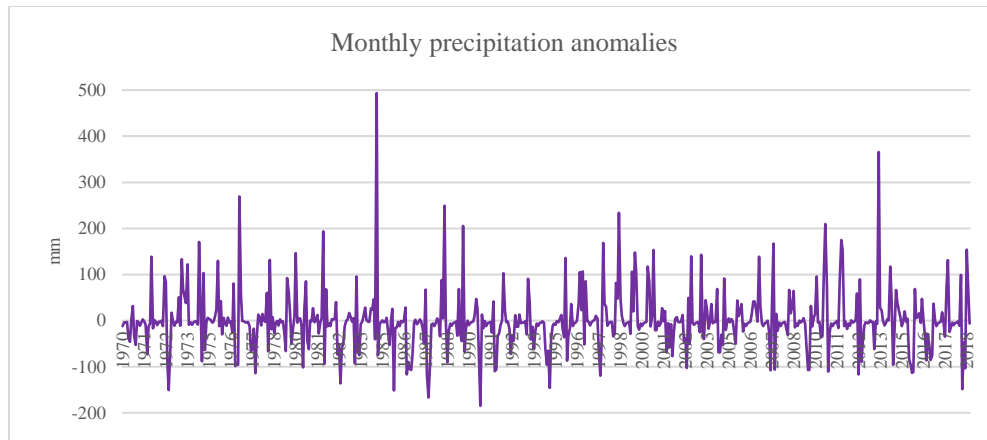


Figure 18. Monthly precipitation anomalies in CPH

In terms of temperature, a trend towards a greater number of positive anomalies was observed. On the one hand, in the maximum temperature, 10.3% of the months in the period 1970-1999 showed values 1°C or less below the average value, while 3.6% recorded values 1°C or more above the average. Between 2000 and 2018, only 1% of the months recorded values lower by 1°C or less than the average maximum temperature, while 11% recorded values higher by 1°C or more than the reported average. In the minimum temperature between 1970 and 1999, 13.9% of the months recorded temperatures 1°C or less below the average, while 2.8% showed temperatures 1°C or more above the average value. For the period 2000-2018, no months were observed with temperatures 1°C or less below the average, while 13.2% of the months showed temperatures 1°C or more above the average value.

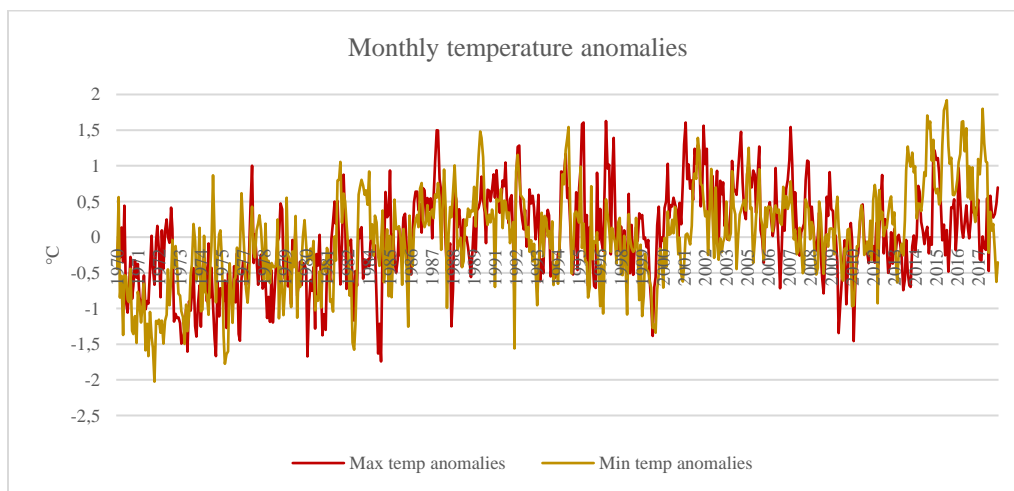


Figure 19. Monthly temperature anomalies in CPH

Dry and rainy days

In this ecoregion there was also a decrease in the average number of dry days compared to those observed in the period 1970-1999. Dry days decreased from 27 to 21 in the rainy season and from 196 to 193 in the dry season. Changes in dry days were identified in the study period, particularly in the dry season, which shows a decreasing trend in dry days compared to the period 1970-1999. In the case of the rainy season, the study period maintained the increasing trend observed between 1979 and 1999.

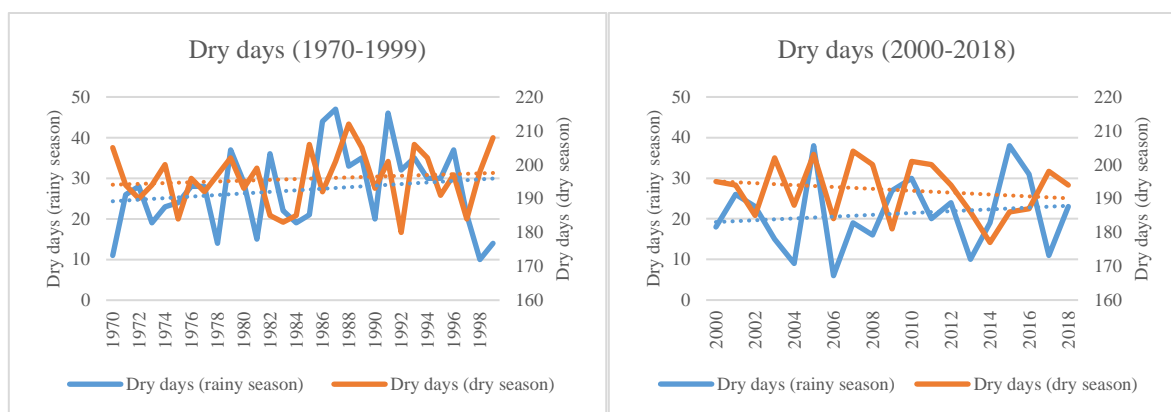


Figure 20. Dry days in CPH

The number of rainy days increased between the two periods. Between 1970 and 1999, the average number of rainy days per year was 126 in the rainy season and 16 in the dry season, while for the period 2000-2018 it was 132 and 20 rainy days, respectively. In the rainy season of the study period, light rainfall accounted for 71%, moderate rainfall 23%, heavy rainfall 5% and thunderstorms (50-100 mm) 1%. In the dry season, light rains accounted for 89%, moderate rains 8.8%, heavy rains 2% and storms 0.3%. The years with the highest number of heavy events in the rainy season were 2005 (11), 2006 (14), 2010 (12) and 2014 (14), while 2007, 2011 and 2013 had the highest number of storms, with two events per year. Also, in 2013, one prolonged storm event was recorded in the rainy season. In the case of the dry season, one storm event was recorded in 2002, while two heavy rain events were observed in each year in 2004 and 2010. Finally, a trend in increasing intensity of dry season rainy days was observed between 2013 and 2018. Compared to the period 1970-1999, in the wet season, a 2% increase in moderate rainfall and a 1% decrease in heavy rainfall days was observed. In the dry season, heavy rainfall increased by 1%.

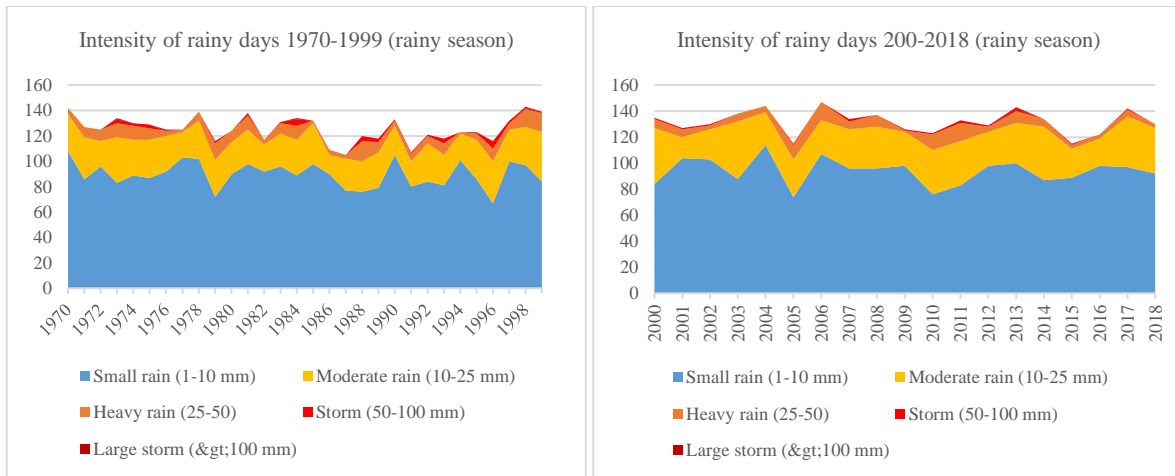


Figure 21. Intensity of rainy days in CPH (rainy season)

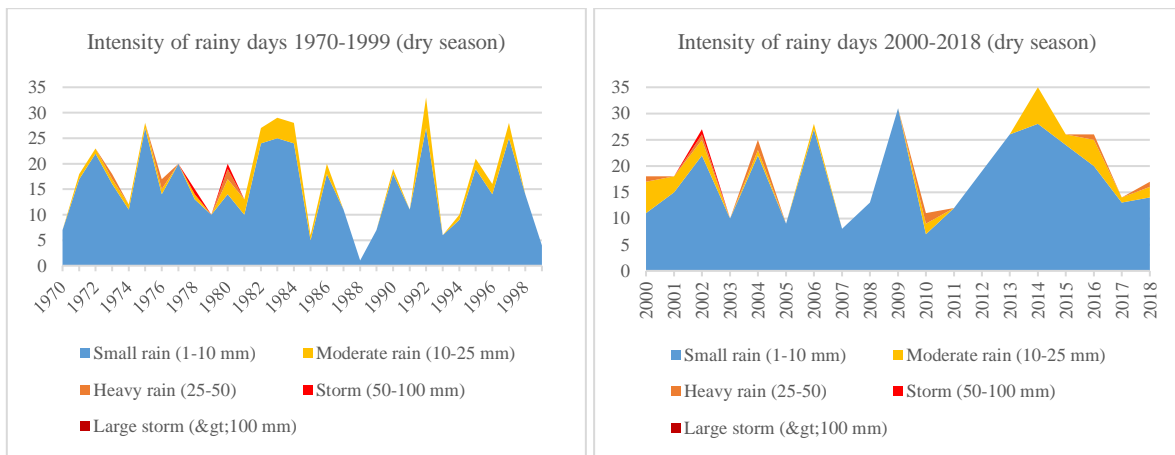


Figure 22. Intensity of rainy days in CPH (dry season)

Droughts and wet events

In the LCP, a transition from drought to wet events was observed between the two periods. Between 1970 and 1999, 78 drought events were identified (2.6 per year), of which 51% were moderate, 46% severe and 3% extreme. Likewise, 51 wet events (1.7 per year) were recorded, of which 53% were moderate, 41% very wet and 6% extremely wet. During the period 2000-2018, 35 drought events (1.7 per year) were observed, of which 97% were moderate and 3% severe, while no extreme drought events were observed. The year with the most intense and prolonged drought was 2002. On the other hand, 48 wet events were recorded (2.5 per year), of which 79% were moderate, 15% very wet and 6% extremely wet. The year with the most intense wet events was 2014, which recorded three extreme wet events and two very wet events. This year was followed by 2000 and 2011 in terms of intensity and duration.

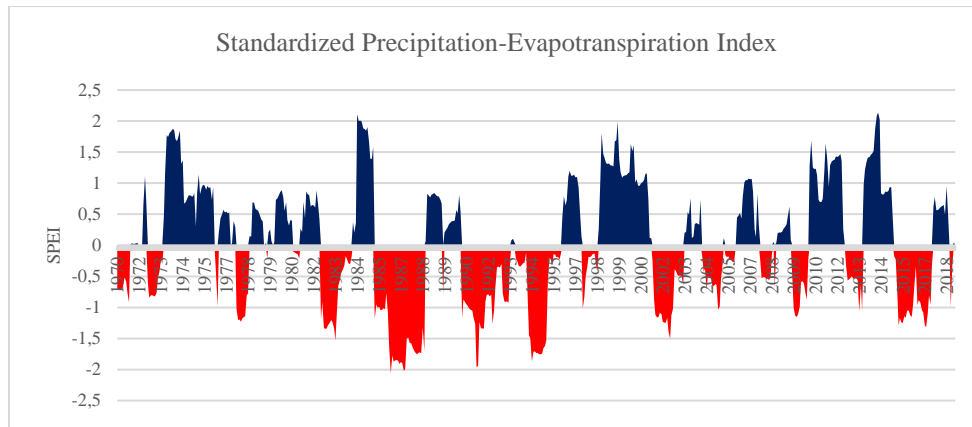


Figure 23. CPH-SPEI

Future climate trajectories

Projections for the PCP under SSP245 showed a 40 mm increase in average annual precipitation for the period 2041-2060. The main increases in precipitation during the rainy season were observed in the months of June and October, with 42 and 59 mm respectively, while a decrease in precipitation of 50 mm is expected in August compared to the study period. During the dry season, the largest variation was observed in the month of May, with expected reductions of 12 mm. On the other hand, projections under SSP585 showed a reduction in annual precipitation of 24 mm for the period 2041-2060 compared to the average value for the study period. The main increase in precipitation was observed in the month of October, with 56 mm, while the main reductions were recorded in August and September, with 34 and 32 mm less than the study period, respectively. In the dry season, the largest variation was recorded in the month of May, with a reduction of 18 mm compared to 2000-2018.

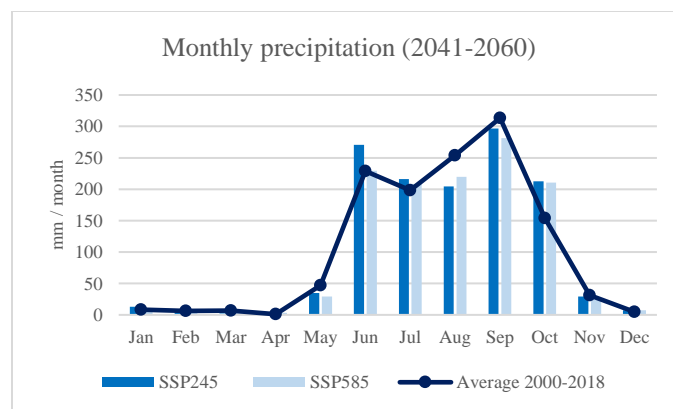


Figure 24. Monthly precipitation in CPH (2041-2060)

Regarding temperature, projections of the maximum temperature under SSP245 for the period 2041-2060 show an increase in the annual average of 2.03°C compared to 2000-2018. Monthly increases

range between 1.3°C and 2.8°C, with March, April, May and December showing the largest increases. On the other hand, projections of the maximum temperature under SSP585 for the period 2041-2060 showed an increase in the annual average of 2.7°C. Monthly increases ranged between 1.8°C and 3.2°C, with March, April, May and August showing the largest increases.

Projections of the minimum temperature under SSP245 showed an increase in the annual average of 1.76°C over the period 2000-2018. Monthly increases range between 0.6°C and 2.7°C, with June, July, August and September showing the largest increases. On the other hand, minimum temperature projections for the period 2041-2060 under SSP585 showed an increase in the annual average of 2.2°C over the study period. Monthly increases ranged between 1°C and 3.35°C, with the months of the rainy season (June-October) showing the largest increases.

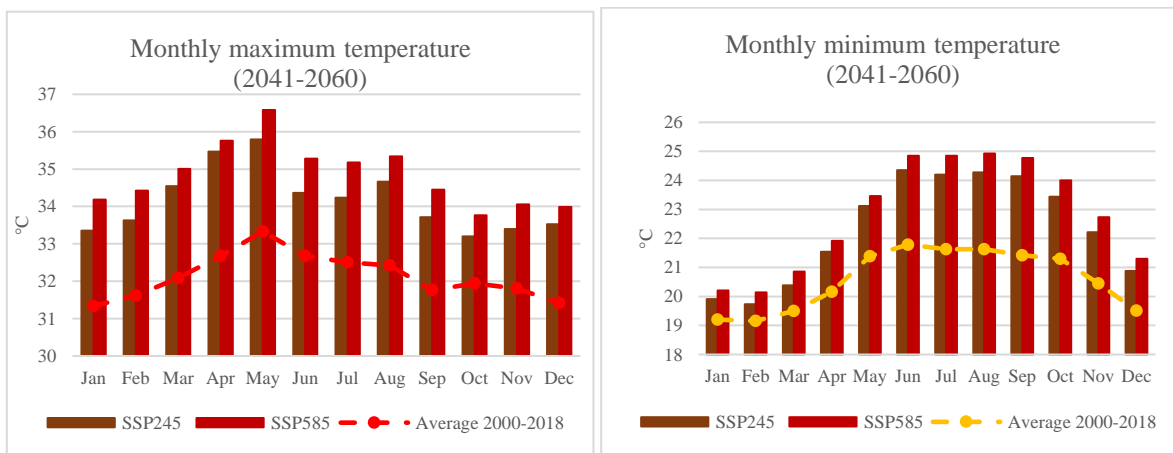


Figure 25. Monthly maximum and minimum temperature in CPH (2041-2060)

4.1.4. Temperate mountain ranges of Sierra Madre del Sur

Precipitation in the SMS has shown an increasing trend. On the one hand, higher levels of annual precipitation have been observed since 2010 compared to those recorded in the first decade of this century. On the other hand, the average annual precipitation for the period 2000-2018 is 200 mm higher than the average observed between 1970 and 1999, which was 1,148 mm per year. This increase is mainly observed during the rainy season, especially in the months of June, July, August and September, with variations of 32 mm to 45 mm per month.

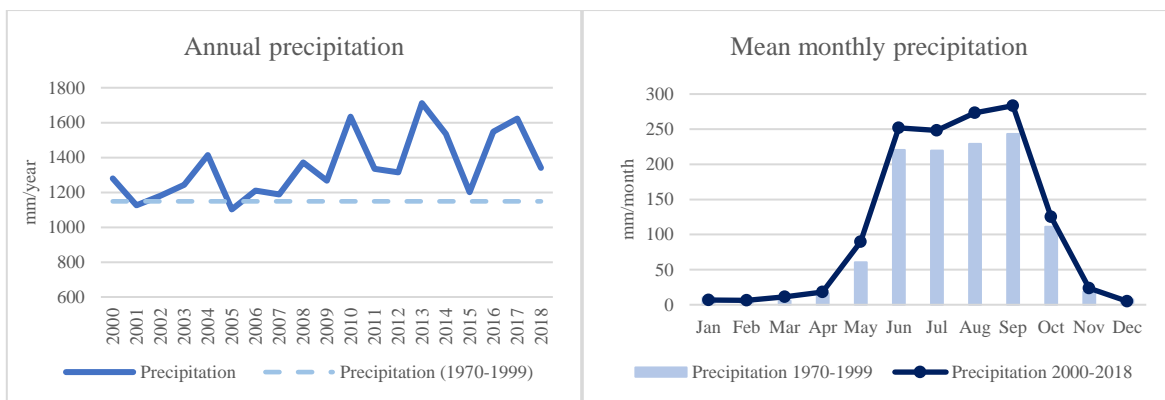


Figure 26. Annual precipitation & mean monthly precipitation in SMS

In terms of temperature, no clear trend is observed during the period 2000-2018 in this ecoregion. During this period, the average maximum temperature has been 0.3°C higher than that recorded between 1970 and 1999. The main increases with respect to this period were observed in the dry season, especially in the months of February, April and May, with increases of 0.5°C, 0.7°C and 0.5°C, respectively. On the other hand, a decrease of 0.6°C in the minimum temperature has been observed compared to that recorded between 1970 and 1999. The decrease in the minimum temperature has been observed in all months of the year, however, the months of November, December and January showed the largest decreases, with changes between -0.8°C and -1.2°C.

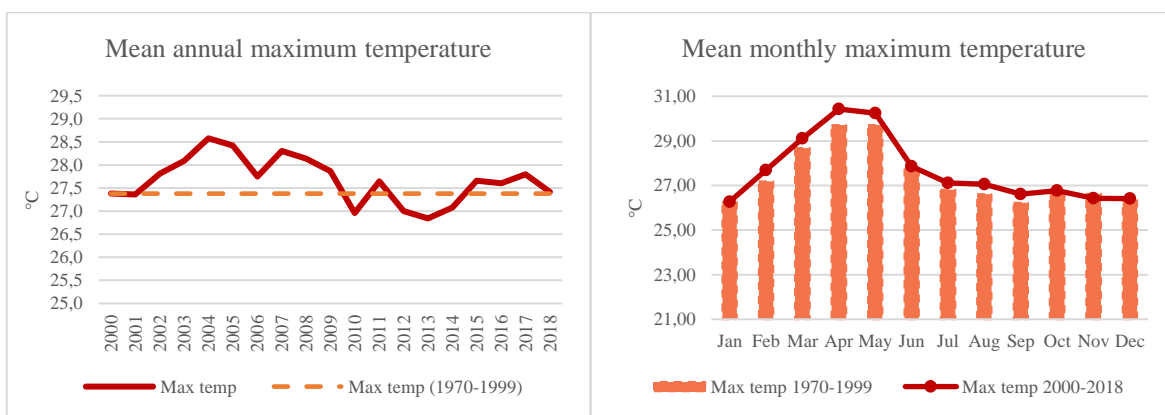


Figure 27. Mean annual maximum temperature & mean monthly maximum temperature in SMS

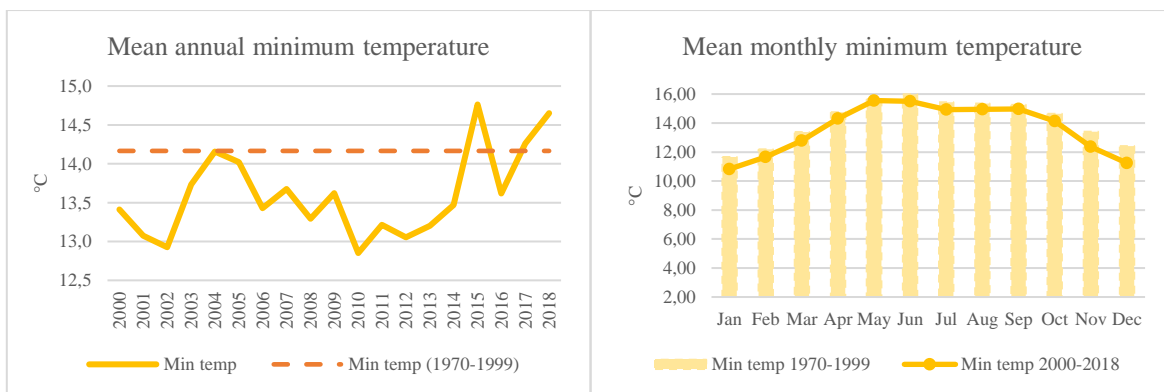


Figure 28. Mean annual minimum temperature & mean monthly minimum temperature in SMS

Anomalies

Precipitation anomalies have changed their behaviour between the two periods. Between 1970 and 1999, it was observed that most of the monthly anomalies had negative values. During this period, 11.9% of the months had rainfall 50 mm or less above average, while 6.1% had rainfall 50 mm or more above average. Between 2000 and 2018, monthly anomalies with positive values were predominant. It was observed that 13.6% of the months exceeded the average monthly values by 50 mm or more, while 4.8% reported values below average values by 50 mm or less.

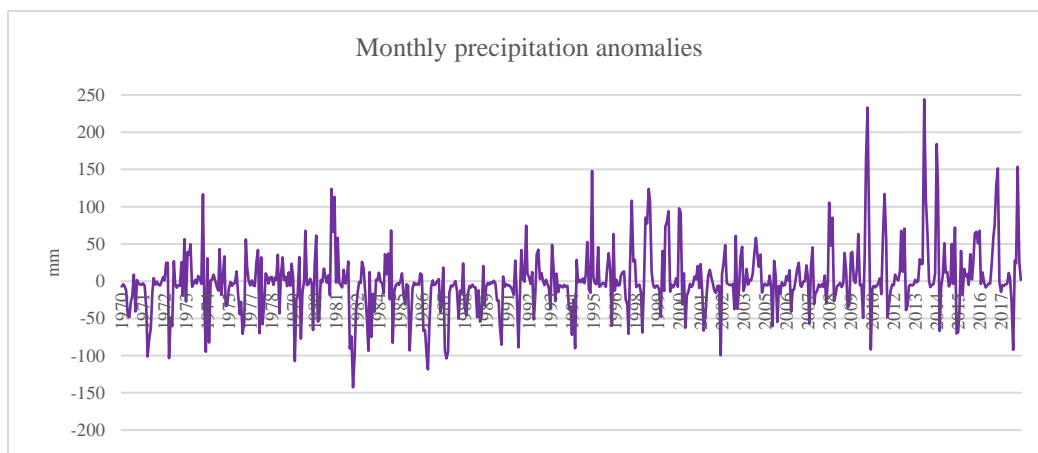


Figure 29. Monthly precipitation anomalies in SMS

There is a trend towards a greater number of positive anomalies in the maximum temperature. 21.1% of the months in the period 1970-1999 showed values 1°C or less below the average value, while 20.6% recorded values 1°C or more above the average. Between 2000 and 2018, 7% of the months recorded values lower by 1°C or less than the average maximum temperature, while 14% showed values higher by 1°C or more than the reported average. On the other hand, in the minimum temperature, between 1970 and 1999, 10.3% of the months recorded temperatures 1°C or less below the average, while 23.9% showed temperatures 1°C or more above the average value. For the period

2000-2018, negative anomalies predominated, as 15.4% of the months recorded temperatures 1°C or less below the average, while 6.6% showed temperatures 1°C or more above the average value.

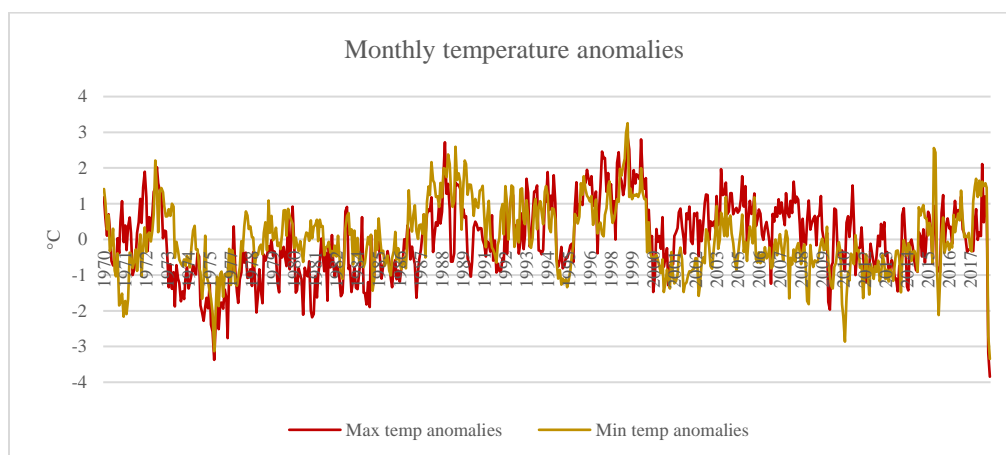


Figure 30. Monthly temperature anomalies in SMS

Dry and rainy days

This is one of the ecoregions with the lowest average number of dry days. A reduction in the average number of dry days was observed between the periods 1970-1999 and 2000-2018, from 13 to 7 days in the rainy season and 178 to 174 in the dry season. The largest change in the trend of dry days between the two periods was observed in the dry season, as the increasing trend observed in 1970-1999 became decreasing in the study period. In the case of the rainy season, the decreasing trend observed in 1970-1999 changed to a stable condition around the average during the study period.

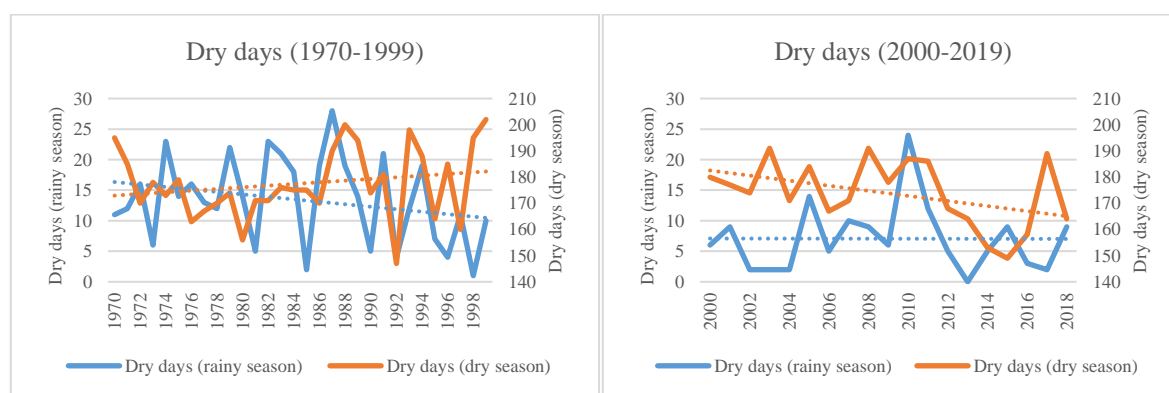


Figure 31. Dry days in SMS

In this ecoregion there was an increase in the number of rainy days between the two periods. Between 1970 and 1999, the average number of rainy days per year was 140 in the rainy season and 35 in the dry season, while for the study period it was 146 and 38 rainy days, respectively. In terms of intensity, in the rainy season of the study period, light (1-10 mm) and moderate (10-25 mm) rainfall accounted

for 70% and 29%, respectively. In the dry season, light rainfall accounted for 94.5%, moderate rainfall 5.2% and heavy rainfall 0.3%. Two heavy rainfall events were recorded in the dry season, one in 2010 and one in 2014. Although no clear trends of change in intensity were observed between 2000 and 2018, an increase in intensity was identified in this period compared to 1970-1999. In the wet season, light events decreased by 4%, while moderate rainfall increased by 4%. In the dry season, light rainfall decreased by 1.7% and moderate rainfall increased by 1.6%.

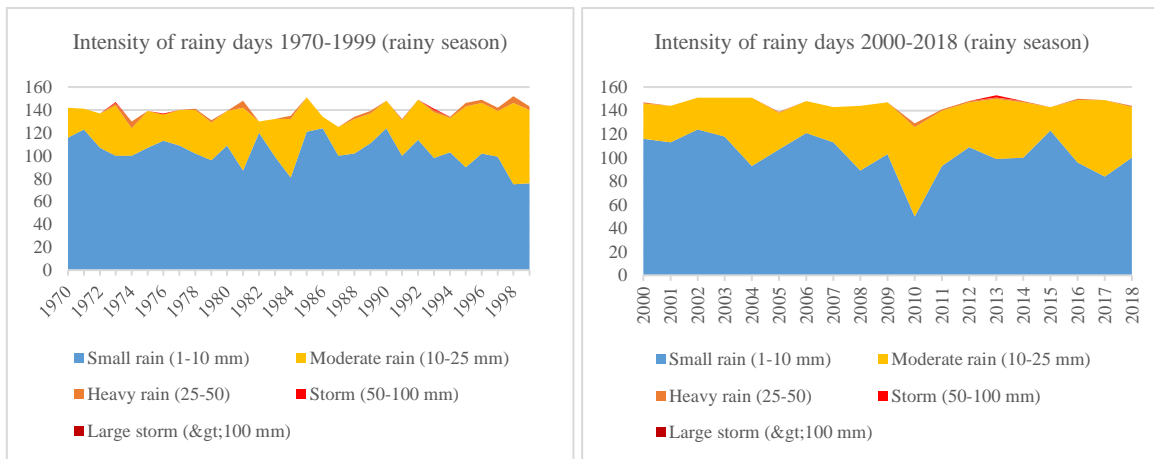


Figure 32. Intensity of rainy days in SMS (rainy season)

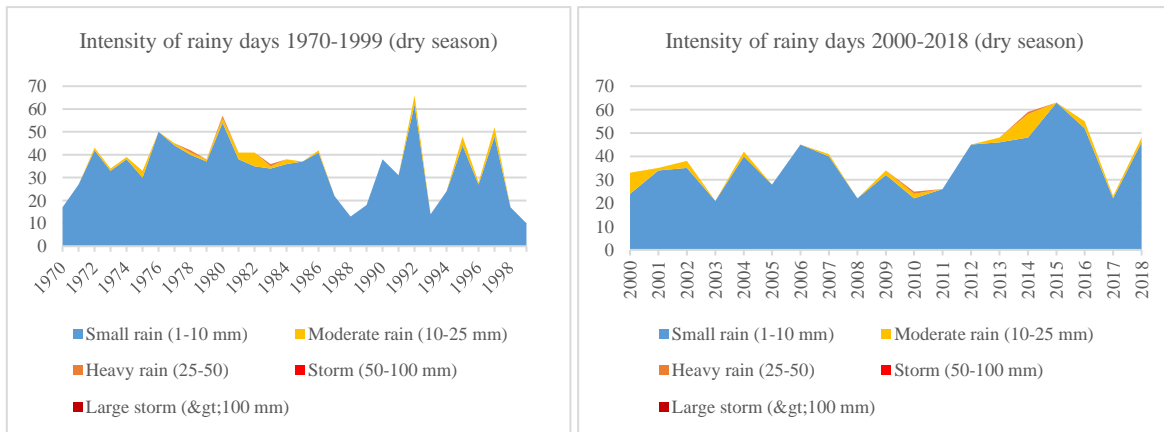


Figure 33. Intensity of rainy days in SMS (dry season)

Droughts and wet events

In the SMS, a transition from droughts to wet events is observed between the two periods. Between 1970 and 2018, 84 drought events were identified (2.8 per year), of which 48% were moderate, 46% severe and 6% extreme. During the period 2000-2018, only five drought events were observed (0.3

per year), of which four were moderate and one severe. The years with these droughts were 2002 and 2005. Between 1970 and 1999, 33 wet events were recorded (1.1 per year), of which 73% were moderate and 27% very wet. No extremely wet events were recorded during this period. In the study period, 62 wet events (3.3 per year) were recorded, of which 47% were moderate, 37% very wet and 16% extremely wet. The years with the most intense wet events were 2010 and 2014.

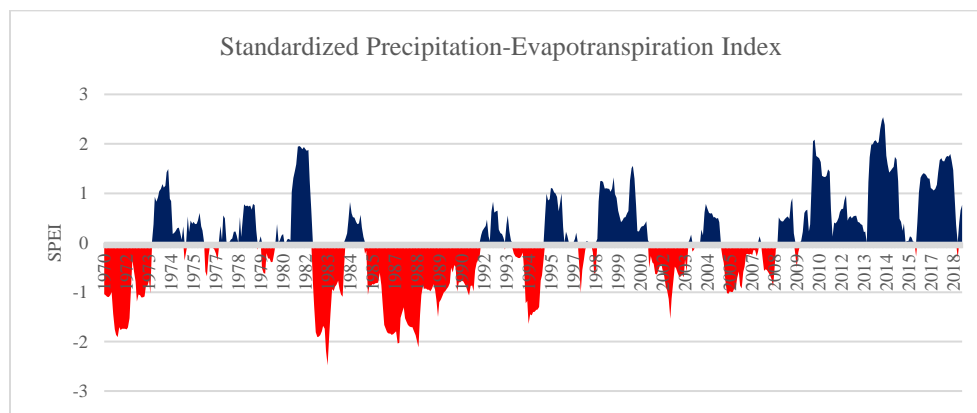


Figure 34. SMS-SPEI

Future climate trajectories

Projections for the SMS under SSP245 showed a 192 mm reduction in average annual precipitation for the period 2041-2060 compared to the average value for the period 2000-2018. The main reductions in precipitation during the rainy season were observed in the months of July, August and September, with -43, -101 and -55 mm respectively, while in October an increase in precipitation of 30 mm is expected over the study period. During the dry season, the largest variation was observed in the month of May, with a reduction in expected precipitation of 27 mm. On the other hand, simulations under SSP585 showed a reduction in annual precipitation of 245 mm for the period 2041-2060 with respect to the average value for the study period. During the rainy season, the main increase in precipitation was observed in the month of October, with 33 mm, while the main reductions were recorded in July, August and September, with -53, -91 and -65 mm, respectively. In the dry season, the largest variation was recorded in the month of May, with a reduction of 35 mm compared to 2000-2018.

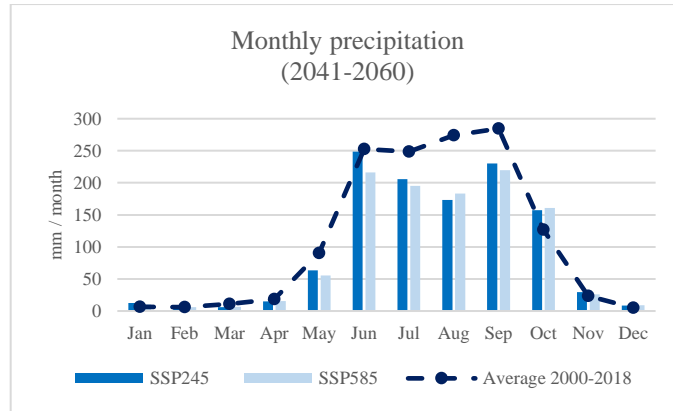


Figure 35. Monthly precipitation in SMS (2041-2060)

The maximum temperature projections under SSP245 showed an increase in the annual average of 2.43°C over the period 2000-2018. Monthly increases ranged between 2°C and 3.1°C, with January, August and September showing the largest increases. On the other hand, maximum temperature projections under SSP585 showed an increase in the annual average of 3.2°C over the study period. Monthly increases ranged between 2.6°C and 3.95°C, with January, August and September being the months where the largest increases were observed.

Projections of the minimum temperature under SSP245 showed an increase in the annual average of 2.9°C over the period 2000-2018. Monthly increases range between 2.3°C and 3.4°C, with July, August, September, October and November showing the largest increases. On the other hand, minimum temperature projections under SSP585 showed an increase in the annual average of 3.5°C over the study period. Monthly increases ranged between 2.7°C and 4°C, with July, August, September, October and November showing the largest increases.

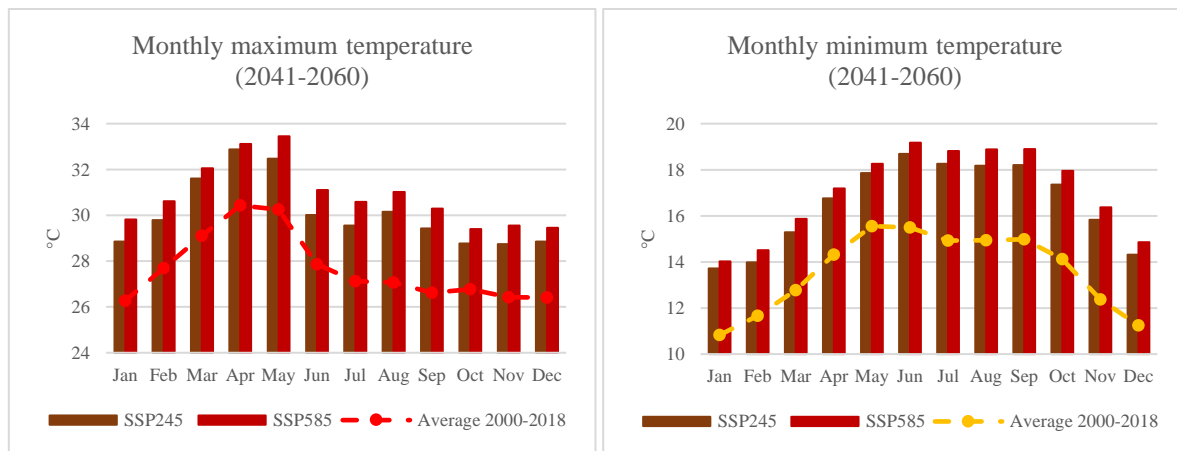


Figure 36. Monthly maximum and minimum temperature in SMS (2041-2060)

4.1.5. Temperate mountain ranges of the Transverse Neovolcanic System

The average annual precipitation in the TNS increased by 90 mm compared to that recorded between 1970 and 1999. Although its distribution between 2000 and 2018 did not show a clear trend, the greatest variations occurred in the transition years between phases. The main changes in precipitation levels between the two periods are observed in the months of May, August and September, the latter being the one with the greatest variation, with an increase of 23 mm.

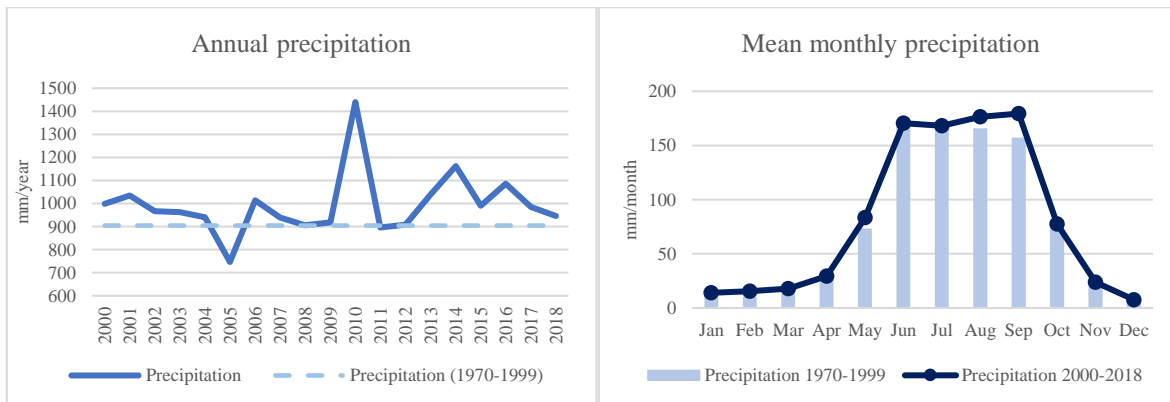


Figure 37. Annual precipitation & mean monthly precipitation in TNS

This ecoregion has shown an increasing trend in temperature. The maximum temperature in the study period does not show clear trends in its behaviour, however, the average recorded is 0.5°C higher than that of the 1970-1999 period. This increase can be observed in the months of February, July and August, with average increases of 0.8°C in each case. On the other hand, the average minimum temperature has shown an increasing trend, both in the study period and in comparison with the average recorded between 1970 and 1999. The observed increase in the average minimum temperature over this period amounted to 0.5°C. The months that reported the greatest increase with respect to the averages observed between 1970 and 1999 were December, January and February, the latter two with increases of more than 1°C.

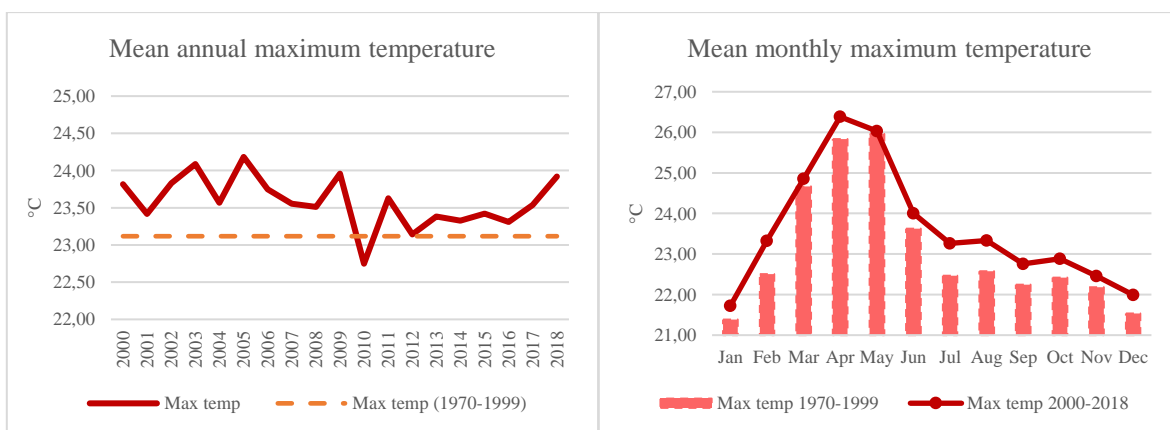


Figure 38. Mean annual maximum temperature & mean monthly maximum temperature in TNS

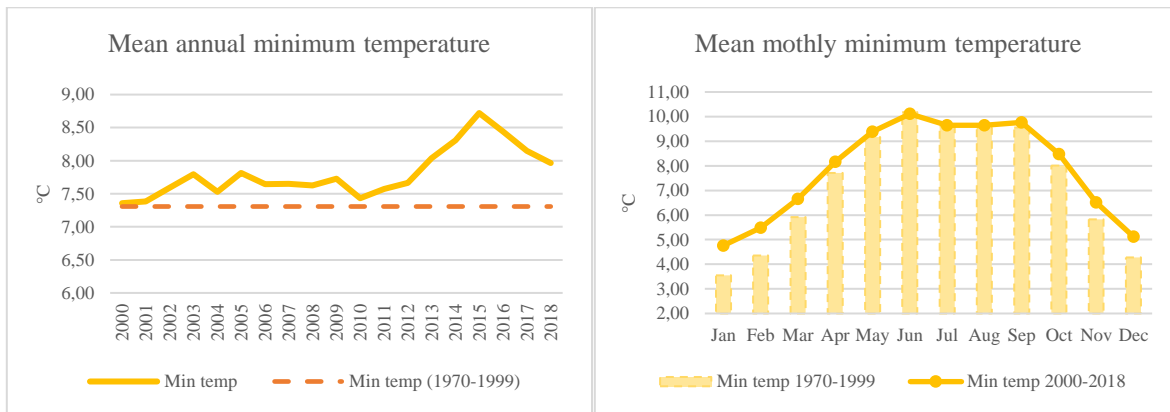


Figure 39. Mean annual minimum temperature & mean monthly minimum temperature in TNS

Anomalies

Precipitation anomalies have changed their behaviour between the two periods. Between 1970 and 1999, it was observed that most of the monthly anomalies had negative values. During this period, 5.6% of the months had rainfall 50 mm or less above average, while 2.8% had rainfall 50 mm or more above average. Between 2000 and 2018, monthly anomalies with positive values predominated. It was observed that 7.9% of the months exceeded the average monthly values by 50 mm or more, while only 2.2% reported values below average values by 50 mm or less.

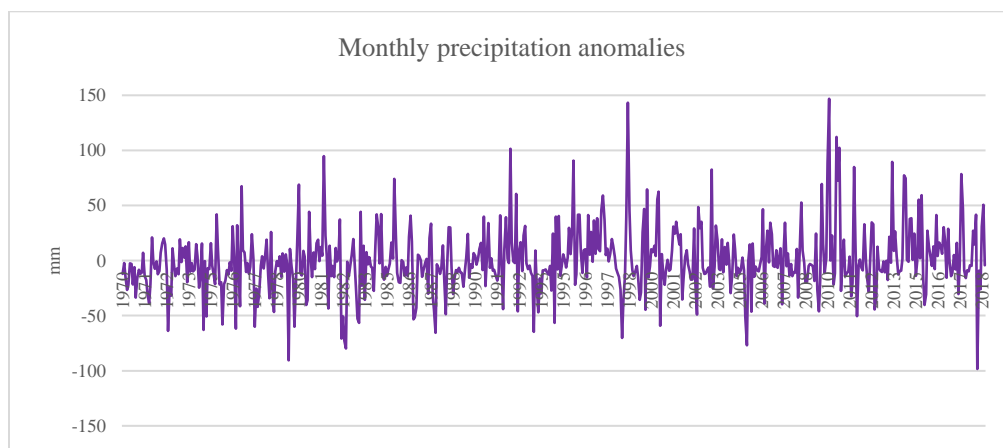


Figure 40. Monthly precipitation anomalies in TNS

In terms of temperature, a trend towards a greater number of positive anomalies was observed. On the one hand, in the maximum temperature, 17.8% of the months in the period 1970-1999 showed values 1°C or less below the average value, while 8.3% recorded values 1°C or more above the average. Between 2000 and 2018, 3.5% of the months recorded values lower by 1°C or less than the average maximum temperature, while 16.2% had values higher by 1°C or more than the reported

average. On the other hand, in the minimum temperature, between 1970 and 1999, 10.3% of the months recorded temperatures 1°C or less below the average, while 3.9% showed temperatures 1°C or more above the average value. For the period 2000-2018, it was observed that only 1% of the months recorded temperatures 1°C or less below the average, while 13.2% showed temperatures 1°C or more above the average value.

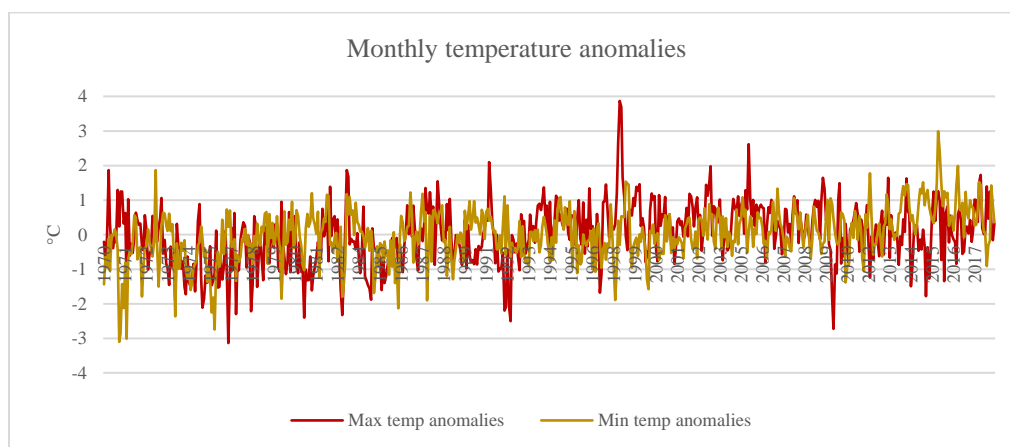


Figure 41. Monthly temperature anomalies in TNS

Dry and rainy days

As in the SMS, this ecoregion recorded low annual averages of dry days. A reduction in the average number of dry days was observed between the periods 1970-1999 and 2000-2018, from 21 to 13 days in the rainy season and 167 to 160 in the dry season. Between 1970 and 1999, in both the rainy and dry seasons, there were decreasing trends in the number of dry days per year. However, these trends changed during the study period, remaining relatively stable in relation to the average for each season. It should also be noted that in 2010 there was an outlier in the behaviour of the dry season, with a minimum of 85 dry days.

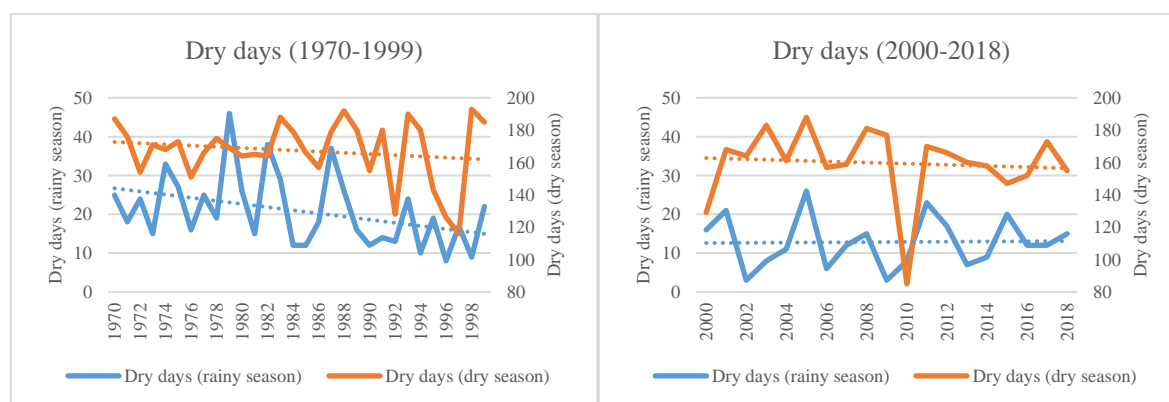


Figure 42. Dry days in TNS

In this ecoregion there was an increase in the number of rainy days between the two periods. Between 1970 and 1999, the average number of rainy days per year was 140 in the rainy season and 35 in the dry season, while for the study period it was 146 and 38 rainy days, respectively. In terms of intensity, in the rainy season of the study period, light (1-10 mm) and moderate (10-25 mm) rainfall accounted for 70% and 29%, respectively. In the dry season, light rainfall accounted for 94.5%, moderate rainfall 5.2% and heavy rainfall 0.3%. Two heavy rainfall events were recorded in the dry season, one in 2010 and one in 2014. Although no clear trends of change in intensity were observed between 2000 and 2018, an increase in intensity was identified in this period compared to 1970-1999. In the wet season, light events decreased by 4%, while moderate rainfall increased by 4%. In the dry season, light rainfall decreased by 1.7% and moderate rainfall increased by 1.6%.

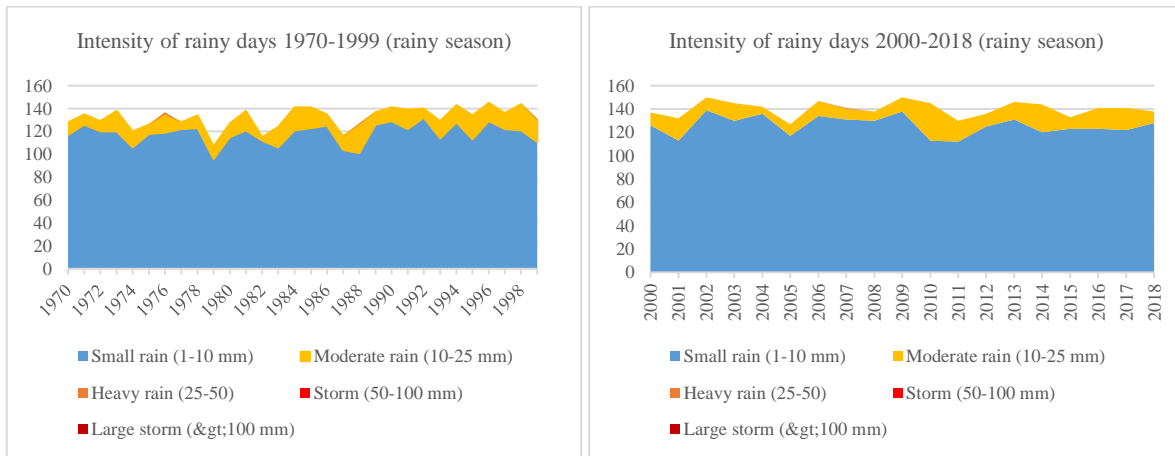


Figure 43. Intensity of rainy days in TNS (rainy season)

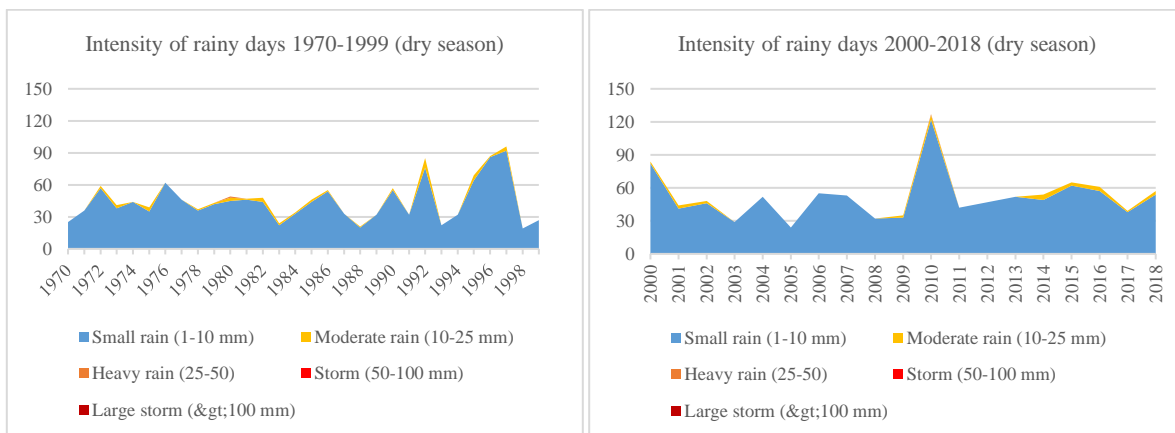


Figure 44. Intensity of rainy days in TNS (dry season)

Droughts and wet events

In the TNS, a transition from droughts to wet events was observed between the two periods. Between 1970 and 2018, 73 drought events were identified (2.4 per year), of which 55% were moderate, 37% severe and 8% extreme. Likewise, 54 wet events were recorded (1.8 per year), of which 72% were moderate and 28% very wet. No extremely wet events were recorded in this ecoregion. During the period 2000-2018, 17 drought events were observed (0.9 per year), of which 41% were moderate, 41% severe and 18% extreme. The years with these droughts were 2005 and 2006. On the other hand, 42 wet events were recorded (2.2 per year), of which 43% were moderate, 36% very wet and 21% extremely wet. The years with the most intense wet events were 2010, 2011 and 2015.

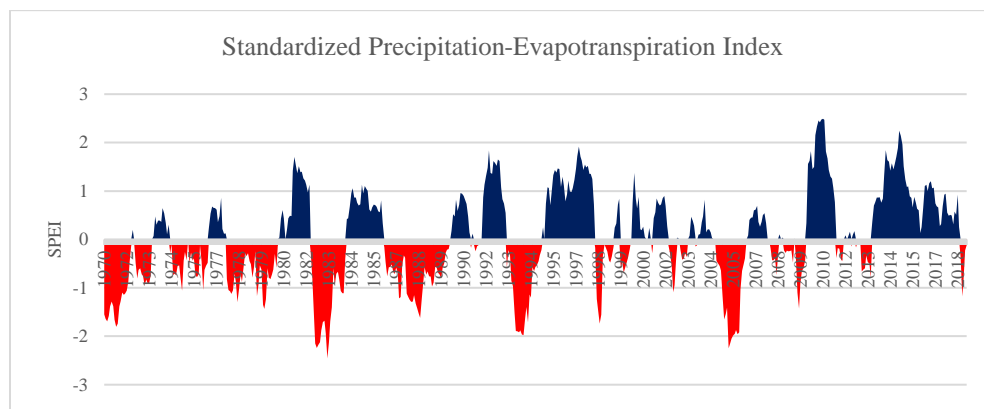


Figure 45. TNS-SPEI

Future climate trajectories

Projections for the TNS under SSP245 showed an increase of 5 mm in average annual precipitation compared to the average value for the period 2000-2018. The main reductions in precipitation during the rainy season are observed in the months of August and September, with -38 and -26 mm respectively, while increases of 67 and 30 mm are expected in June and October, respectively, compared to the study period. During the dry season, the largest variation is observed in the month of May, with a reduction in expected rainfall of 13 mm. On the other hand, projections under SSP585 showed a reduction in annual precipitation of 71 mm compared to the average value for the study period. The main increase in precipitation during the rainy season was observed in the month of October, with 33 mm, while the main reductions were recorded in July, August and September, with -53, -91 and -65 mm compared to the study period, respectively. In the dry season, the largest variation was observed in May, with a reduction of 23 mm compared to 2000-2018.

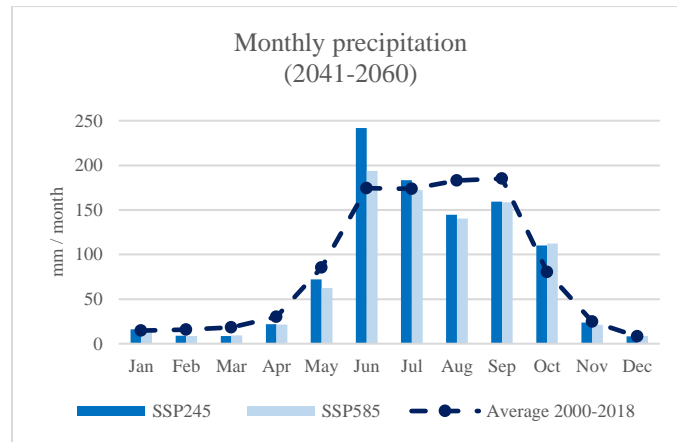


Figure 46. Monthly precipitation in TNS (2041-2060)

The maximum temperature projections under SSP245 showed an increase in the annual average of 2.4°C over the period 2000-2018. Monthly increases ranged between 1.6°C and 3.5°C, with January, March, April and May showing the largest increases. On the other hand, maximum temperature projections under SSP585 showed an increase in the annual average of 3.3°C over the study period. Monthly increases ranged between 2.4°C and 4.05°C, with January, March, April and May showing the largest increases.

Minimum temperature projections under SSP245 showed an increase in the annual average of 2.56°C over the period 2000-2018. Monthly increases ranged between 1.5°C and 3.4°C, with June, July, September, October and November showing the largest increases. On the other hand, minimum temperature projections under SSP585 showed an increase in the annual average of 3.08°C over the study period. Monthly increases ranged between 1.9°C and 3.8°C, with the months of the rainy season (June-October) showing the largest increases.

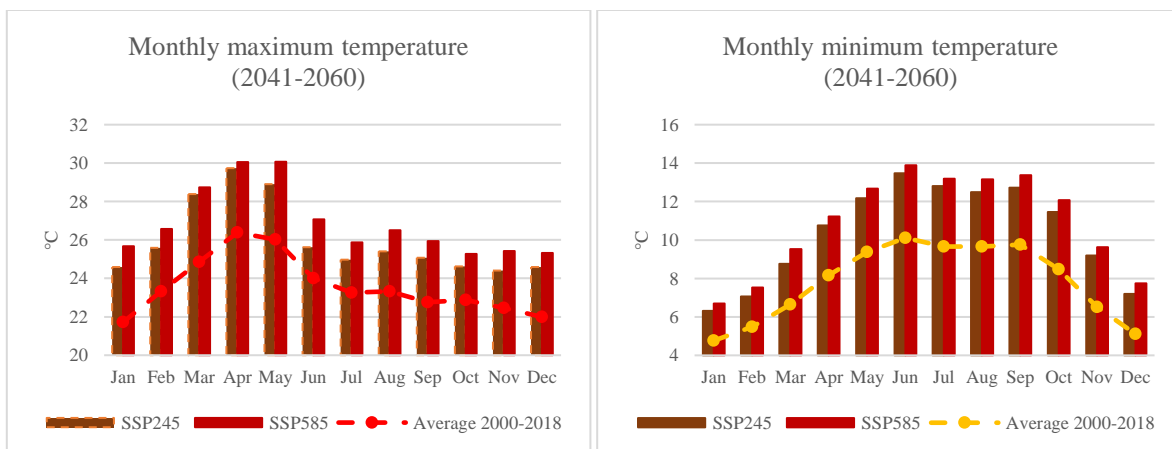


Figure 47. Monthly maximum and minimum temperature in TNS (2041-2060)

4.2. Effects of climate change

4.2.1. Vulnerability to climate change and hazards

Vulnerability to climate change

41% of the municipalities in the BPA have level one vulnerability. This means that they register very high and high vulnerability for at least one of the six vulnerabilities specified in the methodology. They also have increased future vulnerability for at least one vulnerability. Seven per cent have level two vulnerability, which means that they have three vulnerabilities with very high and high degrees, as well as two or more with increased vulnerability in the future. Four per cent of the municipalities in the ABS were categorised with vulnerability level three, which means that they have four or more vulnerabilities with high and very high categories, as well as two or more with future increase. Most of the municipalities with high levels of vulnerability (second and third level) are located south of the LCPs, in the Costa Chica region of Guerrero and the coast of Oaxaca; south of the SMS, in the La Montaña region of Guerrero and the southern Sierra of Oaxaca; in the IDs between the states of Michoacán and Guerrero; and in the northwest of the TNS, between the states of Michoacán and Jalisco.

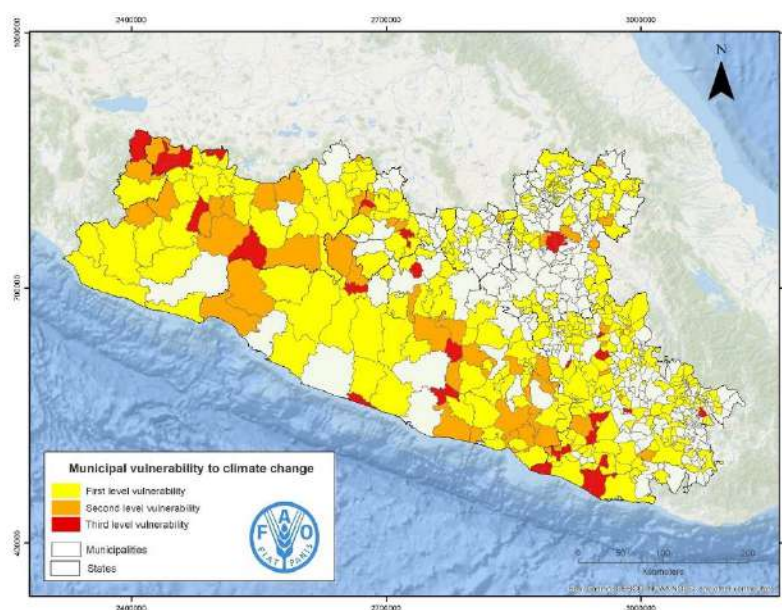


Figure 48. Municipal vulnerability to climate change in BALSAS area project (INECC, 2019)

Drought, flood, tropical cyclone and frost hazards and risks

Droughts, floods, tropical cyclones and frost are the main hydrometeorological phenomena affecting the rural and urban population of the BPA. According to CENAPRED, 30% of the municipalities of the BPA have a low degree of danger due to drought, 55% have a moderate degree, 13% a high degree

and 1% a very high degree. The municipalities with the greatest danger due to drought are located in the Michoacán and Puebla DIs, the Michoacán and Oaxaca PCPs, as well as in the Michoacán and Oaxaca SMS. In terms of flooding, 3% of the municipalities have a low risk level, 25% moderate and 3% high. Most of the municipalities with the highest level of risk are located in the PCP of Guerrero, Michoacán and Oaxaca, as well as the DI of Michoacán, Guerrero, Morelos and Puebla. Regarding tropical cyclone risk, only 5% of the municipalities in the basin present moderate to very high levels of risk, however, these represent the majority of the municipalities in the PCP, the SMS and DI of the region of La Montaña de Guerrero, as well as the municipalities of the DI between Michoacán and Guerrero. Finally, 68% of the municipalities in the BPA have low or very low, 26% moderate and 7% high frost hazard levels. The vast majority of the municipalities with the highest degree of frost danger are located in the TNS, particularly in the north of the states of Michoacán, Mexico, Puebla and Tlaxcala.

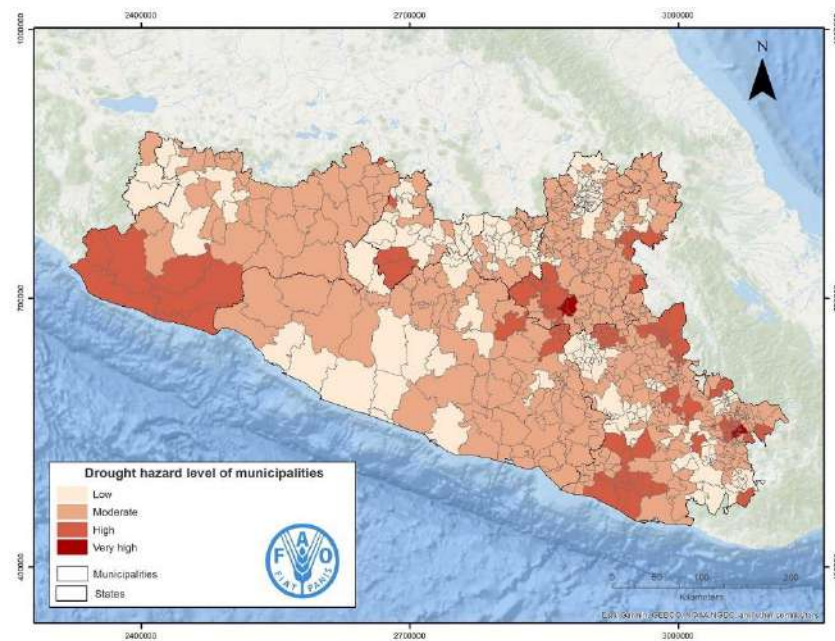


Figure 49. Drought hazard level of municipalities (CENAPRED, 2012)

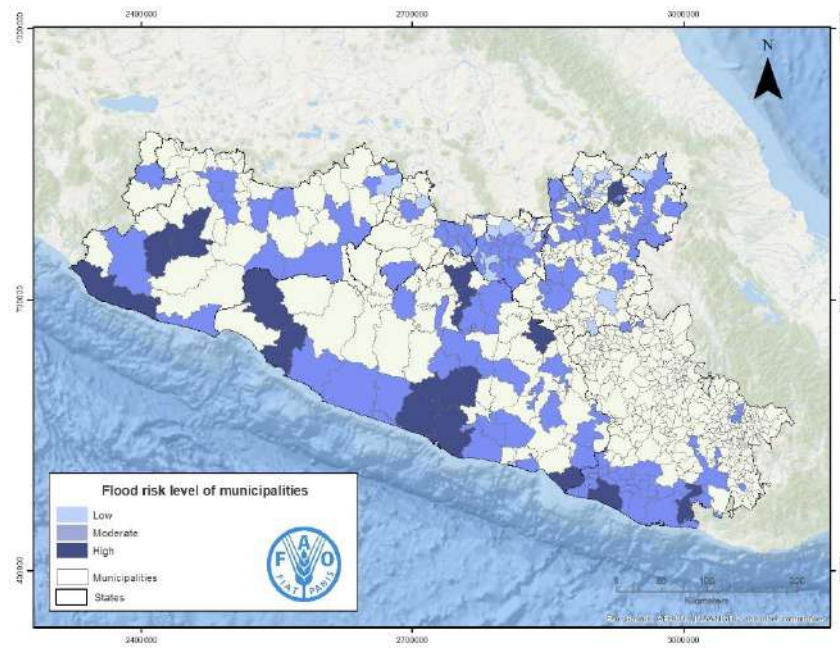


Figure 50. Flood risk level of municipalities (CENAPRED, 2016)

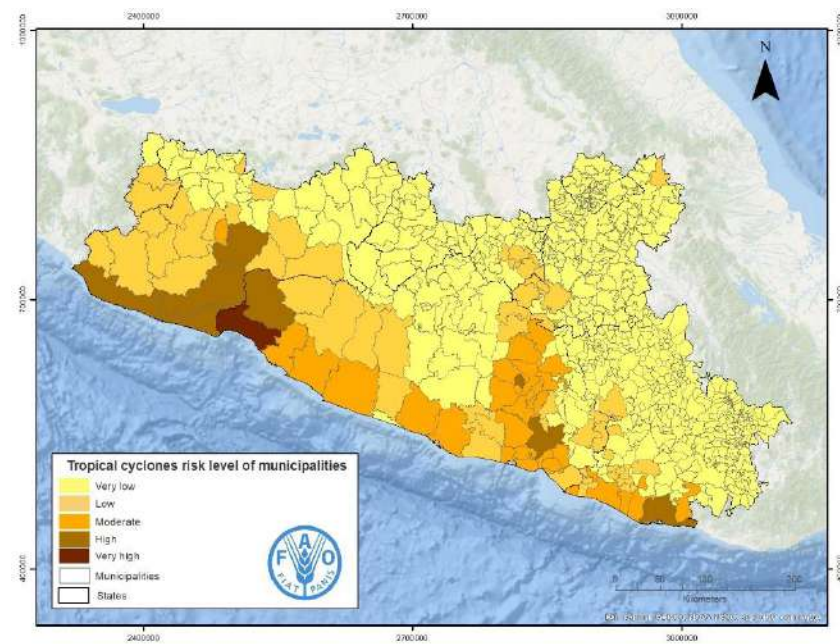


Figure 51. Tropical cyclones risk level of municipalities (Montealegre Zúñiga & Matías Ramírez, 2021)

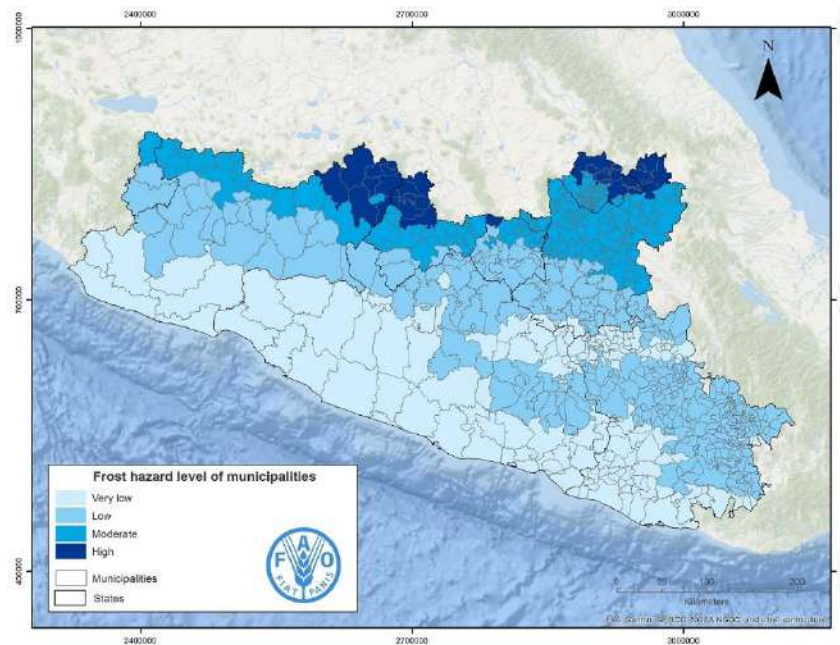


Figure 52. Frost hazard level of municipalities (Vidal-García, 2007)

4.2.2. Disasters

Droughts

During the period 2000-2018, 1,337 emergency and disaster declarations due to drought were registered in the BPA. The municipalities that registered the highest number of declarations for these phenomena were located in the DI and the PCP. Ninety-five per cent of these events were recorded between 2000 and 2009. The years with the highest number of declarations for this phenomenon were 2002, 2003, 2005 and 2009. In 2002, 311 declarations were recorded, most of which were issued at the beginning or during the rainy season and ended at the end of the rainy season and the beginning of the dry season. With respect to ENSO dynamics, during this period the transition from the neutral phase to El Niño was observed, which is associated with dry events during the rainy season in the study area. In 2003, 135 emergency and disaster declarations were issued due to drought, which were effective in September and October. During this period, ENSO dynamics were in a neutral phase. In 2005, 269 drought emergency and disaster declarations were registered, 89% of which started in April and May, the months corresponding to the dry season. However, in most cases, their duration extended into September and even November. In 2005, ENSO dynamics were in transition from

neutral to La Niña. In that sense, the combined effects of both phases can be associated with dry events during the rainy season and extend into the dry season at the end of the year. In 2009, 216 warnings were recorded, most of which were issued at the beginning of the rainy season and remained in effect until August and September. The ENSO dynamics for this period were in transition from La Niña to El Niño, so the dry events are attributed to this phenomenon. Finally, one aspect to highlight is that only 55 declarations were issued in 2015, a year in which there was a canonical El Niño, whose effects in terms of droughts were not as intense because the ITTA did not cross the Equator.

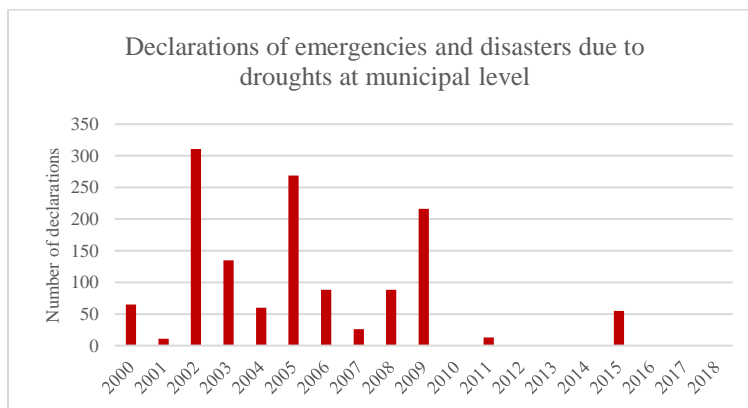


Figure 53. Declarations of emergencies and disasters due to droughts at municipal level (CENAPRED, sf)

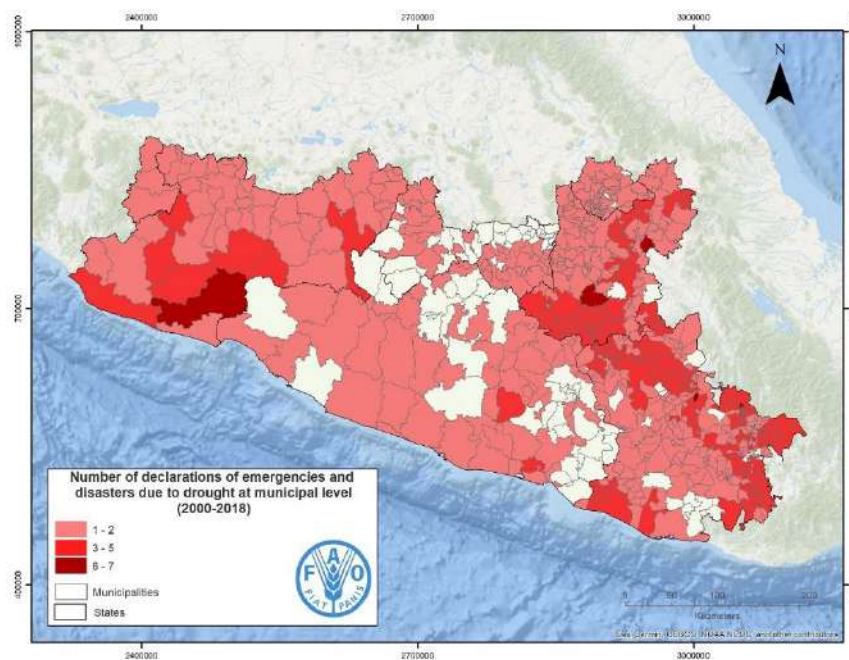


Figure 54. Map of declarations of emergencies and disasters due to droughts at municipal level 2000-2018 (CENAPRED, sf)

Floods and rains

During the period 2000-2018, 870 declarations of emergencies and disasters due to floods and atypical rains were registered in the BPA. The municipalities with the highest number of declarations for these phenomena were located in the PCP and SMS. Two thirds of these events were recorded between 2010 and 2018. The years with the highest number of declarations for this phenomenon were 2007, 2010, 2014 and 2017. In 2007, 90 warnings were issued in three monthly periods: May (7), July (13) and August (70). The ENSO dynamics during these periods, corresponding to the rainy season, correspond to La Niña, whose effects are observed in the increase in rainfall during the rainy season. In 2010, 144 emergency and disaster declarations were issued for floods and atypical rains in five monthly periods, of which two correspond to the dry season: January (29), February (75); and three to the rainy season: July (11), August (22) and September (7). During this period, ENSO dynamics were in a transition phase from El Niño, characterised by intense rainfall effects in the dry season, to La Niña, characterised by intense precipitation events in the rainy season. In 2014, 119 warnings were issued in three monthly periods, most of them at the beginning of the rainy season: June (112), July (1) and September (6). The ENSO dynamics during these periods corresponds to the neutral phase. In 2017, 167 warnings were issued in three periods: one during the dry season in March (4) and two during the rainy season, in June (42) and September (121). The ENSO dynamics for this period were in the La Niña phase, so rainfall in the rainy season was more intense.

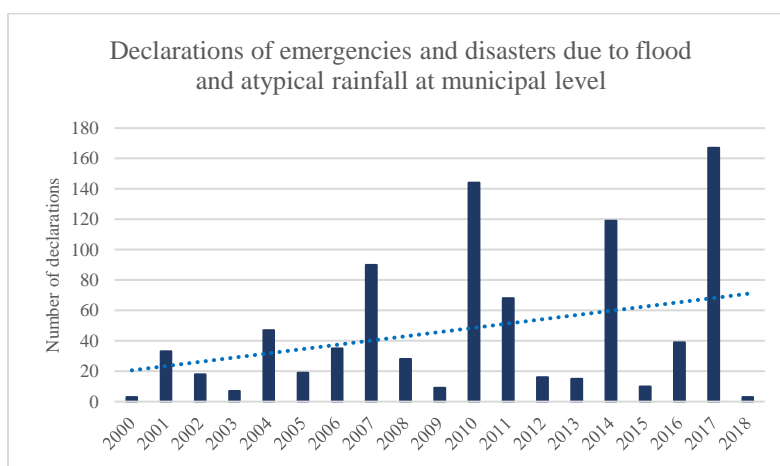


Figure 55. Declarations of emergencies and disasters due to flood & atypical rain at municipal level (CENAPRED, sf)

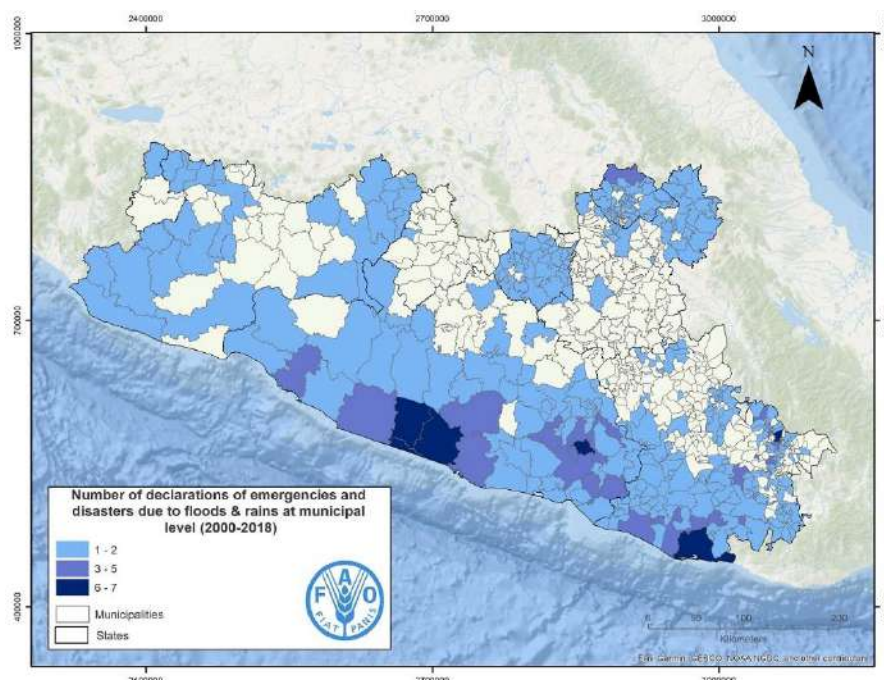


Figure 56. Map of declarations of emergencies and disasters due to flood & atypical rain at municipal level (CENAPRED, sf)

Tropical cyclones

During the period 2000-2018, 2,090 declarations of emergencies and disasters due to tropical cyclones were registered in the BPA. The municipalities that registered the highest number of declarations for these phenomena were located in the PCP and SMS. Eighty-two per cent of the declarations were registered in five years: 2000, 2005, 2012, 2013 and 2014. In 2000, 760 declarations were issued, the highest number recorded during the study period. This atypical number of declarations can be associated with the occurrence of two tropical storms (Norman and Rosa) that made landfall in the areas of the BPA where the municipalities with the highest risk of tropical cyclones are located (CONAGUA^{a,b}, 2000). During these months, ENSO dynamics were in the La Niña phase. Although this ENSO phase is mainly associated with the presence of tropical cyclones in the Atlantic Ocean, both Norman and Lane originated in the Pacific. In 2005, 172 declarations were issued for four tropical cyclones, 98% of which were due to the temporary convergence of Hurricane Stan and Tropical Wave 40 in October. Hurricane Stan originated in the Atlantic and developed during the La Niña phase. In 2012, 207 declarations were recorded for the effects of Hurricane Carlotta (144), formed in the Pacific, and Tropical Storm Ernesto (63), formed in the Atlantic, in June and August, respectively. During these months, ENSO dynamics were in the neutral phase. The neutral phase of ENSO prevailed during 2013, a year in which 408 declarations were issued for three tropical cyclones: Hurricane Manuel (2) in August, the combined effect of Hurricanes

Ingrid and Manuel (392) in September, and Hurricane Raymond (14) in October. In 2014, 171 declarations were issued, 96% of which corresponded to the effects of tropical storm Trudy in October. In this month, ENSO dynamics were in the neutral phase.

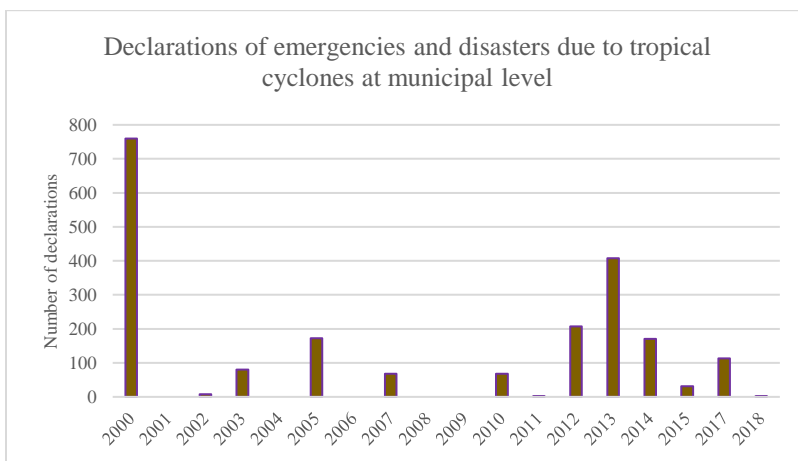


Figure 57. Declarations of emergencies and disasters due to tropical cyclones at municipal level (CENAPRED, n.d.)

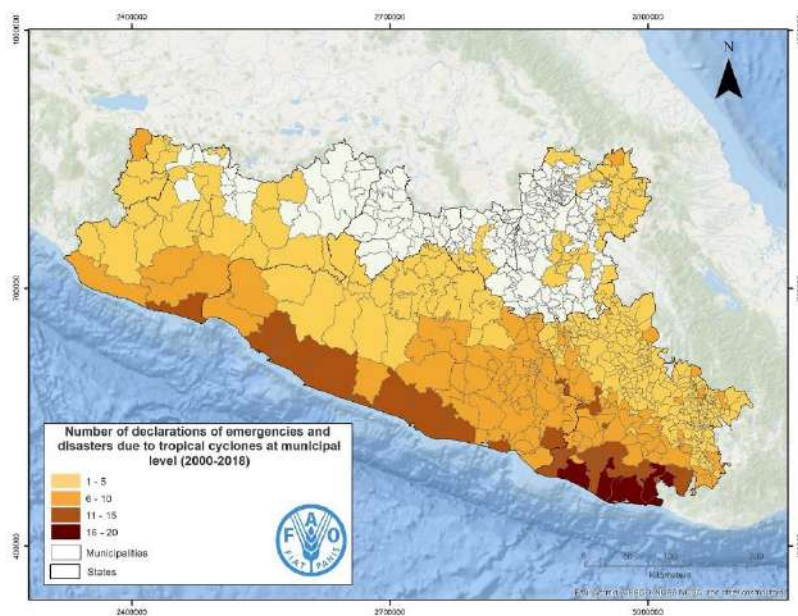


Figure 58. Map of declarations of emergencies and disasters due to tropical cyclones at municipal level (CENAPRED, n.d.)

Hail, snow and frost

During the period 2000-2018, 612 declarations of emergencies and disasters due to hail, snowfall and frost were registered in the BPA. The municipalities that registered the highest number of declarations for these phenomena were located in the TNS. Six years accounted for 77% of the declarations: 2000, 2001, 2006, 2011, 2014 and 2016. In 2000, 35 declarations were issued in the month of July, the month in which the La Niña phase was developing. In 2001, 217 declarations were issued, the highest number recorded in the period. The declarations were issued in December, during the neutral phase of the ENSO dynamic. In 2006, 48 warnings were recorded, of which 32 were issued in January, while the rest were issued between June and September. In this year, La Niña events were recorded in January, and the transition between the neutral phase and El Niño in the months of the rainy season. The above shows atypical behaviour with respect to the events expected due to ENSO dynamics. In 2011, 64 warnings were issued in May, June and September, with the latter accounting for the majority (55 warnings). During this period, the La Niña phase was developing, which is associated with higher humidity in the rainy season. In 2014, 38 warnings were recorded, of which 30 were issued in January and the rest in July, while the neutral phase of ENSO dynamics was developing. Finally, in 2016, 61 declarations were issued in January and February. The El Niño phase occurred during these months.

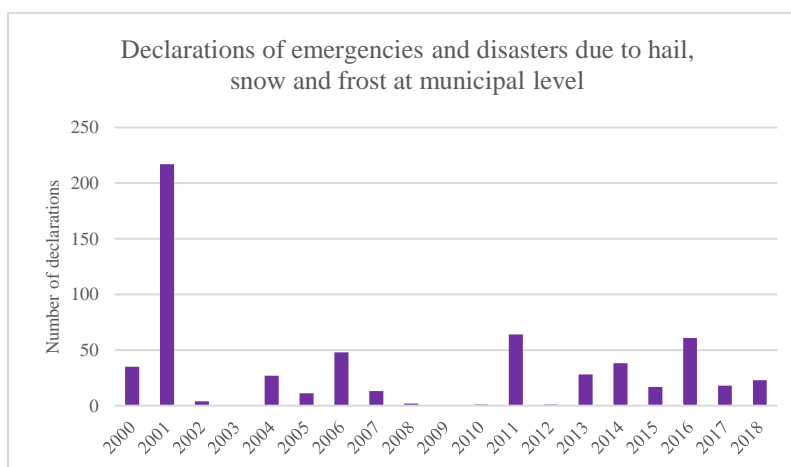


Figure 59. Declarations of emergencies and disasters due to hail, snow & frost rain at municipal level (CENAPRED, sf)

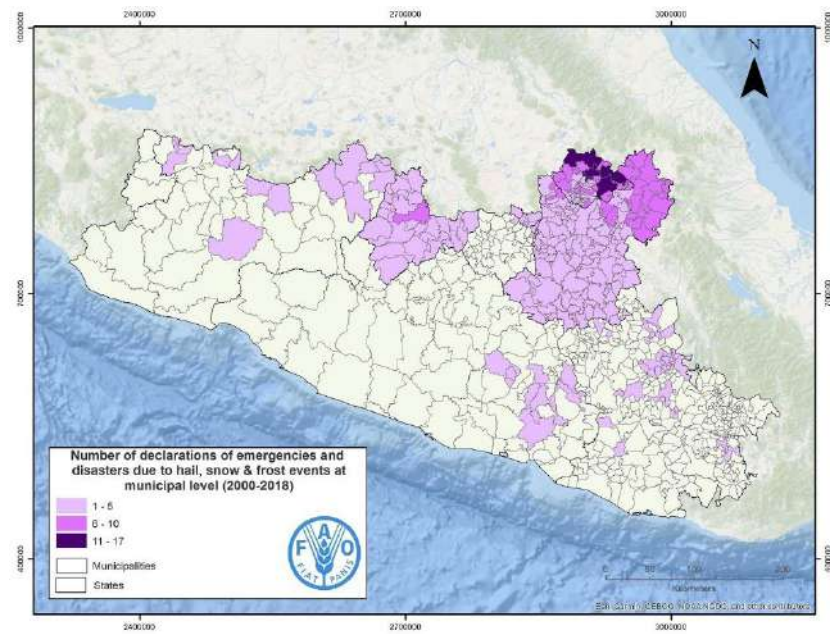


Figure 60. Map of declarations of emergencies and disasters due to hail, snow & frost rain at municipal level (CENAPRED, sf)

5. Conclusions

The results showed evidence of the effects of climate change and climate variability in the BPA ecoregions. These effects consist of: increased temperature patterns, as well as changes in precipitation trends, frequency and intensity of dry/wet events, and impacts of extreme events. Globally, the impact of climate change on climate variability has been documented through increased frequency and intensity of more extreme weather events (Thornton et al., 2014; IPCC, 2012). According to the IPCC (2012), there is evidence that changes in observed climate extremes since 1950 are due to anthropogenic drivers. As discussed in the introduction, while it is true that the intensification of climate variability and extreme events associated with ENSO dynamics are associated with climate change effects, the separation between mean changes (climate change) and changes in variability with respect to their contribution to the occurrence of extreme weather events is currently unknown (van der Wiel & Bitanjia, 2021). Therefore, the effects of this intensification in climate variability in the BPA were observed from the declarations of emergencies and disasters due to droughts, rains and floods, tropical cyclones, as well as frost and hail.

With regard to temperature, the results obtained show a trend towards an increase in temperature in the study area. Despite this generalized increase, the observed changes vary according to the ecoregion, while in the PCP and TNS an increase in maximum and minimum temperatures is observed, in the DI and SMS the maximum temperature has increased, while the minimum temperature has decreased. Given that any long-term variation in temperature has a significant impact on crop production (Mohammed & Tarpley, 2011), the observed results are of great relevance to a region like the BPA, where most of the rural population's livelihoods depend on agriculture. According to Mohammed & Tarpley (2011), temperature alters enzyme function within a leaf and causes changes in the growth and development stages of the crop, leading to reduced yields. In the case of minimum temperature, several studies have addressed the effects of increased minimum temperature (night temperature) on crop physiology, which alters leaf enzyme function, decreases photosynthetic function, increases respiration rate, suppresses flower bud development, accelerates crop maturity, which causes a decrease in yields (Mohammed & Tarpley, 2011; Loka & Oosterhuis, 2010; Mohammed & Tarpley, 2009a; Mohammed & Tarpley, 2009^b; Turnbull et al., 2002). Based on these effects, concerns about increasing temperature trends are heightened when considering that future simulations project increases of 2 to 3.6°C in annual average maximum temperature and 1.76 to 4°C in minimum temperature for the period 2041-2060 under fossil fuel-intensive trend development scenarios.

Similarly, an increasing trend in precipitation was observed in the BPA ecoregions between 2010 and 2018 with respect to the average of the reference period 1970-1999. This trend became more pronounced from 2010 onwards. The months with the greatest increase in precipitation correspond to the rainy season. This trend of increasing precipitation has also been reported for all of Mexico in the Sixth National Communication to the United Nations Framework Convention on Climate Change (SEMARNAT-INECC, 2018). It has been widely documented that changes in precipitation are closely related to ENSO dynamics (Yun et al., 2021; Xie et al., 2010; Magaña et al., 2003). In this case, the results show an association between increases in precipitation levels and the cold and neutral phases of ENSO, which predominated during the study period. These results are consistent with those reported by Pinilla Herrera and Pinzón Correa (2016) for the mountainous area of the BPA.

In addition to the increase in precipitation, a transition from a dry to a wet phase was observed between the periods 1970-1999 and 2000-2018. A clear transition from negative to positive precipitation anomalies was observed in three ecoregions (DI, SMS and TNS), except in the LCPs, where the ratio between both types of anomalies was maintained between the two periods. According to the annual climate report (CONAGUA, 2018) show the trend towards the prevalence of positive precipitation anomalies during the period 2000-2018 in Mexico, which contributes to the robustness of the results obtained. Also, the transition between dry and wet days was observed in the four ecoregions, as while in the period 1970-1999 dry days prevailed, between 1999 and 2018 wet days predominated. This condition of prevalence of wet days in the study period was accompanied by an increase in rainfall intensity in the PCP, SMS and TNS.

There is a pattern in the frequency and intensity of dry/wet days and climate variability associated with ENSO behavior. In this sense, higher levels of precipitation, rainy days, were observed during the rainy season and an increase in the intensity of rainy days during La Niña and the neutral phase. Likewise, an increase in drought events was observed in the rainy season during the El Niño phase.

It was observed that more than half of the municipalities in the BPA have some level of vulnerability to climate change. The distribution of these municipalities does not follow any specific pattern in terms of ecoregions. In the case of hazards and risks due to hydrometeorological events, these do show patterns associated with the ecoregions. The municipalities located in the PCP and DI have a higher level of danger due to drought, while those located in the TNS have a higher level of danger due to frost. The municipalities located in the PCP and SMS have a higher level of risk from tropical cyclones than the rest of the ecoregions, while the PCP and DI have a higher level of risk from floods.

The effects of climate variability, as well as climate change, can be observed in the occurrence of emergencies and disasters due to climatic phenomena. The most notorious patterns of the effects of climate change and variability can be seen in disaster declarations due to droughts and floods. In the case of drought declarations, these were most frequent between 2000 and 2009, as was the El Niño phase. However, between 2010 and 2018, La Niña and the neutral phase predominated, resulting in fewer drought declarations, but more declarations for floods and atypical rains. In the case of tropical cyclone declarations, there is an association between the months in which the declarations were issued and the presence of La Niña and the neutral phase. These results can be approached from the perspective of climate variability, but also as part of the effects of climate change. Regarding the frost, hail and snowfall declarations, these mainly developed during La Niña, in the months of the rainy season, and the neutral phase of ENSO and El Niño in the months of the dry season. This condition affects the crop production of the rural population, particularly those whose crops are subsistence or family-based cash crops, without access to insurance and living in poverty (Ramírez-Huerta et al., 2013). The variability observed in anomalies and dry/wet events is associated with ENSO dynamics, which can increase or decrease the occurrence of extreme events and the consequent impact on agriculture (Pinilla Herrera and Pinzón Correa, 2016; Jozami et al., 2015). The results obtained are consistent with those reported by Murray-Tortarolo (2020), who observed that the increase (change in intensity) in recent heavy rains, storms, floods and droughts are a consequence of climate change and are likely to be exacerbated in the future.

References

- Alward, R.D., Detling, J.K. & Milchunas, D.G. (1999). Grassland Vegetation Changes and Nocturnal Global Warming. *Science*, 283, 229-231, ISSN 0036-8075
- Andrews, M. B., Ridley, J. K., Wood, R. A., Andrews, T., Blockley, E. W., Booth, B., et al. (2020). Historical simulations with HadGEM3-GC3.1 for CMIP6. *Journal of Advances in Modeling Earth Systems*, 12, e2019MS001995. <https://doi.org/10.1029/2019MS001995>
- Blanco-Macías, F., Magallanes-Quintanar, R., Márquez-Madrid, M., Cerano-Paredes, J., Martínez-Salvador, M. & Valdez-Cepeda, R.D. (2020) Relationship between El Niño Southern Oscillation and Mexico's orange yield anomalies. *Terra Latinoamericana* 38: 827-832. DOI: <https://doi.org/10.28940/terra.v38i4.582>
- Bojinski, S., Verstraete, M., Peterson, T., Richter, C., Simmons, A. & Zemp, M. (2014). The Concept of Essential Climate Variables in Support of Climate Research, Applications, and Policy. *Bulletin of the American Meteorological Society*. 95. 1431. 10.1175/BAMS-D-13-00047.1.
- CENAPRED (2007). Degree of flood risk by municipality, scale: 1:200000. 1 ed. 1 ed. Centro Nacional de Prevención de Desastres. Retrived from: http://www.conabio.gob.mx/informacion/metadatos/gis/grinundmgw.xml?_httpcache=yes&_xsl=/db/metadatos/xsl/fgdc_html.xsl&_indent=no
- CENAPRED (2012). Degree of risk due to tropical cyclones by municipality, scale: 1:200000. 1 ed. National Centre for Disaster Prevention. Retrived from: http://www.conabio.gob.mx/informacion/metadatos/gis/rcictropgw.xml?_httpcache=yes&_xsl=/db/metadatos/xsl/fgdc_html.xsl&_indent=no
- CENAPRED (2012). Grado de peligro por sequía por municipio', scale: 1:20000. 1 ed. Centro Nacional de Prevención de Desastres. Retrived from: http://www.conabio.gob.mx/informacion/metadatos/gis/pelsequigw.xml?_httpcache=yes&_xsl=/db/metadatos/xsl/fgdc_html.xsl&_indent=no
- CENAPRED (2012). Degree of danger for days with frost by municipality, scale: 1:200000. 1 ed. National Centre for Disaster Prevention. Retrived from: http://www.conabio.gob.mx/informacion/metadatos/gis/gpdhelmgw.xml?_httpcache=yes&_xsl=/db/metadatos/xsl/fgdc_html.xsl&_indent=no
- CONAGUA (sf). Hydrological information system. Retrived from: <https://sih.conagua.gob.mx/>

CONAGUA^a (2000) Tropical Storm Norman. Tropical Cyclones 2000. Retrived from: <https://smn.conagua.gob.mx/tools/DATA/Ciclones%20Tropicales/Ciclones/2000-Norman.pdf>

CONAGUA^b (2000) Tropical Storm Rosa. Tropical Cyclones 2000. Retrived from: <https://smn.conagua.gob.mx/tools/DATA/Ciclones%20Tropicales/Ciclones/2018-Rosa.pdf>

Cubasch, U., D. Wuebbles, D. Chen, M.C. Facchini, D. Frame, N. Mahowald, and J.-G. Winther, 2013: Introduction. In: Climate Change (2013). The Physical Science Basis. Contribution of Working Group I to the Fifth Assessment Report of the Intergovernmental Panel on Climate Change [Stocker, T.F., D. Qin, G.-K. Plattner, M. Tignor, S.K. Allen, J. Boschung, A. Nauels, Y. Xia, V. Bex and P.M. Midgley (eds.)]. Cambridge University Press, Cambridge, United Kingdom and New York, NY, USA.

DOFa. AGREEMENT that establishes the guidelines of the Programme for the Response to Emergencies caused by Natural Hazards. Official Journal of the Federation, 16/08/2021.

DOFb. AGREEMENT issuing the Specific Operating Guidelines to address damage caused by disruptive natural phenomena. Official Journal of the Federation, 13/08/2021.

EPA (sf). Climate change indicators in the United States. United States Environmental Protection Agency. Retrived from <https://www.epa.gov/climate-indicators>

Escalante Sandoval, C. & Reyes, L. (2005). Análisis de Sequías [Book]. - [s.l.] : Faculty of Engineering. UNAM,

Feingold, J.S. (2011). El Niño, La Niña, and ENSO. In: Hopley, D. (eds) Encyclopedia of Modern Coral Reefs. Encyclopedia of Earth Sciences Series. Springer, Dordrecht. https://doi.org/10.1007/978-90-481-2639-2_74

Huckelba, A. L., & Van Lange, P. A. M. (2020). The Silent Killer: Consequences of Climate Change and How to Survive Past the Year 2050. *Sustainability*, 12(9), 3757. MDPI AG. <http://dx.doi.org/10.3390/su12093757>

National Institute of Ecology and Climate Change (INECC) (2021). Municipalities Vulnerable to Climate Change based on the results of the National Atlas of Vulnerability to Climate Change.

INEGI-CONABIO-INE (2007). Terrestrial Ecoregions of Mexico. Escala 1:1000000. Retrived from <http://www.conabio.gob.mx/informacion/gis/>

IPCC (2012). Managing the risks of extreme events and disasters to advance climate change adaptation. In: CB Field, V Barros, TF Stocker, et al., editors. A Special Report of Working Groups I and II of the Intergovernmental Panel on Climate Change. Cambridge, NY, USA: Cambridge University Press.

IPCC (sf). Climate change widespread, rapid, and intensifying, Retrived from <https://www.ipcc.ch/2021/08/09/ar6-wg1-20210809-pr/>

Jia, Q., Li, M. & Dou, X. (2022) Climate Change Affects Crop Production Potential in Semi-Arid Regions: A Case Study in Dingxi, Northwest China, in Recent 30 Years. Sustainability, 14, 3578. <https://doi.org/10.3390/su1406357>

Jiménez Espinosa, M., Baeza Ramírez, C., Matías Ramírez, G. L., & Eslava Morales, H. (2012). Mapas de índices de riesgo a escala municipal por fenómenos hidrometeorológicos. CENAPRED.

Jiménez Espinosa, M., Matías Ramírez, L. G., & Eslava Morales, H. (2009). Mapas de riesgo a escala municipal por inundaciones y bajas temperaturas. CENAPRED.

Kellstedt, P.M., Zahran, S., Vedlitz, A. (2008). Personal efficacy, the information environment, and attitudes toward global warming and climate change in the United States. Risk Anal. Int. J., 28, 113-126.

Loka, D.A., Oosterhuis, D.M., 2010. Effect of High Night Temperatures on Cotton Respiration. ATP Levels, and Carbohydrate Content. Environmental and Experimental Botany, Vol. 68, pp. 258-263, ISSN 0098-8472.

Magaña, V., Vázquez, J., Pérez, J. & Pérez, J. (2003) Impact of El Niño on precipitation in Mexico, Geofís. Int., 42, 313-330.

Melgarejo, A.E., Ordoñez, P., Nieto, R., Peña-Ortiz, C., García- Herrera, R. & Gimeno, L. (2021) Mechanisms for Severe Drought Occurrence in the Balsas River Basin (Mexico). Atmosphere, 12, 368. <https://doi.org/10.3390/atmos12030368>

Mohammed, A. R. , & Tarpley, L. (2011). Effects of High Night Temperature on Crop Physiology and Productivity: Plant Growth Regulators Provide a Management Option. In (Ed.), Global Warming Impacts - Case Studies on the Economy, Human Health, and on Urban and Natural Environments. IntechOpen. <https://doi.org/10.5772/24537>

Mohammed, A.R. & Tarpley, L. (2009) High nighttime temperatures affect rice productivity through altered pollen germination and spikelet fertility. Agricultural and Forest Meteorology, 149, 999-1008.

Montealegre Zúñiga, D. & Matías Ramírez, L.G. (2021). Identification of hazards and risks at municipal level to provide basic information for the subsequent development of municipal atlases throughout the country. Floods. Subdirección de riesgos por inundación, CENAPRED.

Moore, C.E., Meacham-Hensold, K., Lemonnier, P., Slattery, R.A., Benjamin, C., Bernacchi, C.J., Lawson, T., Cavanagh, A.P., & Hancock, R. (2021) The effect of increasing temperature on crop photosynthesis: from enzymes to ecosystems. *Journal of Experimental Botany* 72(8). <https://doi.org/10.1093/jxb/erab090>

Moustakis, Y., Onof, C.J. & Paschalis, A. (2020) Atmospheric convection, dynamics and topography shape the scaling pattern of hourly rainfall extremes with temperature globally. *Commun Earth Environ* 1, 11. <https://doi.org/10.1038/s43247-020-0003-0>

NOAA^a (n.a.) <https://psl.noaa.gov/enso/mei/>

NOAA^b (n.d). Cold & Warm Episodes by Season. https://origin.cpc.ncep.noaa.gov/products/analysis_monitoring/ensostuff/ONI_v5.php

Nunes, L. J. R., & Ferreira Dias, M. (2022). Perception of Climate Change Effects over Time and the Contribution of Different Areas of Knowledge to Its Understanding and Mitigation. *Climate*, 10(1), 7. MDPI AG. <http://dx.doi.org/10.3390/cli10010007>

Pinheiro, H.R., Ambrizzi, T., Hodges, K.I. & Gan, M.A. (2022) Understanding the El Niño Southern Oscillation Effect on Cut-Off Lows as Simulated in Forced SST and Fully Coupled Experiments. *Atmosphere*, 13, 1167. <https://doi.org/10.3390/atmos13081167>

Pinilla Herrera, M.C. & Pinzón Correa, C.A. (2016) An assessment of El Niño and La Niña impacts focused on monthly and seasonal rainfall and extreme dry/precipitation events in mountain regions of Colombia and Mexico, *Adv. Geosci.*, 42, 23-33, <https://doi.org/10.5194/adgeo-42-23-2016>.

Poveda, G. & Mesa, O.J. (1996). The extreme phases of the ENSO phenomenon (El Niño and La Niña) and its influence on the hydrology of Colombia. *Hydraulic Engineering in Mexico* 11:1.

Qian, L., Zhu, Q., Zheng, J., Liao, K. & Guishan, Y. (2014). Soil moisture response to rainfall in forestland and vegetable plot in Taihu Lake Basin, China. *Chinese Geographical Science*. 25. [10.1007/s11769-014-0715-0](https://doi.org/10.1007/s11769-014-0715-0).

Ramírez-Huerta, Mónica, Juárez-Sánchez, J.P., Ramírez-Valverde, B. & Ramírez-Valverde, G. (2013). Impact of frost losses on Mexican agriculture and their relationship with rural poverty: case of the state of Puebla. *Juyyaania*, 1:1.

Riahi K., van Vuuren D.P., Kriegler E., Edmonds J., O'Neill B., Fujimori S., Bauer N., Calvin K., Dellink R., Fricko O., Lutz W., Popp A., Cuaresma C.J., Samir K., Leimbach M., Jiang L., Kram T., Rao S., Emmerling J., Ebi K., Hasegawa T., Havlik P., Humpenöder F., Da Silva L.A., Smith S., Stehfest E., Bosetti V., Eom J., Gernaat D., Masui T., Rogelj J., Strefler J., Drouet L., Krey V., Luderer G., Harmsen M., Takahashi K., Baumstark L., Doelman J., Kainuma M., Klimont Z., Marangoni G., Lotze-Campen H., Obersteiner M., Tabeau A., Tavoni M. The shared socioeconomic pathways and their energy, land use, and greenhouse gas emissions implications: an overview. *Glob. Environ. Change*. 2016;42

SEMARNAT-INECC (2018). Mexico. Sixth National Communication and Second Biennial Update Report to the United Nations Framework Convention on Climate Change. Ministry of Environment and Natural Resources - National Institute of Ecology and Climate Change. Retrived from: <https://cambioclimatico.gob.mx/sexta-comunicacion/>

Thornton, P. K., Ericksen, P. J., Herrero, M., & Challinor, A. J. (2014). Climate variability and vulnerability to climate change: a review. *Global change biology*, 20(11), 3313-3328. <https://doi.org/10.1111/gcb.12581>

Trenberth, K.E. (2006) Shea, D.J. Atlantic hurricanes and natural variability in 2005. *Geophys. Res. Lett*, 33, L12704

Turnbull, M.H.; Murthy, R. & Griffin, K.L. (2002). The Relative Impacts of Daytime and Night-time Warming on Photosynthetic Capacity in *Populus deltoides*. *Plant Cell and Environment*, Vol. 25, pp. 1729-1737, ISSN 0140-7791.

Valencia-Vargas, J. C. (2015). Development of the Balsas Hydrological Region through the modification of its closure. *Tecnología y Ciencias del Agua*, 6(1), 81-97.

Valera, V. (2013). Capacity building programme in the formulation of proposals for accessing climate finance. Module 5 Climate Rationality. United Nations Development Programme - UNDP Ecuador.

van der Wiel, K., Bintanja, R. (2021). Contribution of climatic changes in mean and variability to monthly temperature and precipitation extremes. *Commun Earth Environ* 2(1). <https://doi.org/10.1038/s43247-020-00077-4>

Vicente-Serrano, S. M., Beguería, S., & López-Moreno, J. I. (2010). A Multiscalar Drought Index Sensitive to Global Warming: The Standardized Precipitation Evapotranspiration Index, *Journal of Climate*, 23(7), 1696-1718.

Vidal R. & García V. (2007). Amenazas climáticas: Nevadas históricas I y II, carta NA-XIV-6, en sección Naturaleza [Book Section] / book auth. Mexico New National Atlas of Mexico, UNAM. - scale 1:16,000,000. - ISBN: 978-970-32-5047-9.

Wengel, C., Lee, SS., Stuecker, M.F. et al. (2021) Future high-resolution El Niño/Southern Oscillation dynamics. *Nat. Clim.* *Nat. Clim.* 11, 758-765. <https://doi.org/10.1038/s41558-021-01132-4>

WorldClim (sf). Future climate data. Retrived from: <https://www.worldclim.org/data/cmip6/cmip6climate.html>

Xie, S.-P. et al. (2010). Global warming pattern formation: sea surface temperature and rainfall. *J. Clim.* 23, 966-986.

Yun, KS., Lee, JY., Timmermann, A. *et al.* (2021). Increasing ENSO-rainfall variability due to changes in future tropical temperature-rainfall relationship. *Commun Earth Environ* 2, 43. <https://doi.org/10.1038/s43247-021-00108-8>

Zhang, T., Hoell, A., Perlwitz, J., Eischeid, J., Murray, D., Hoerling, M., & Hamill, T. M. (2019). Towards probabilistic multivariate ENSO monitoring. *Geophysical Research Letters*, 46 <https://doi.org/10.1029/2019GL083946>

ANNEX 1. List of weather stations

Intermonane depressions							
C12001	C12077	C12177	C16051	C16241	C17018	C20118	C21063
C12004	C12082	C12210	C16085	C16244	C17020	C20151	C21082
C12007	C12084	C12259	C16109	C17001	C17021	C20202	C21087
C12008	C12091	C15046	C16122	C17003	C17024	C20209	C21165
C12014	C12092	C15195	C16133	C17004	C17026	C20258	C21176
C12018	C12105	C15275	C16136	C17005	C17028	C20266	C21205
C12019	C12110	C15324	C16158	C17006	C17029	C20507	C21217
C12023	C12114	C15346	C16192	C17007	C17031	C21003	C21231
C12030	C12115	C16006	C16219	C17008	C17033	C21007	
C12031	C12116	C16007	C16228	C17012	C17036	C21012	
C12046	C12118	C16026	C16230	C17013	C20034	C21024	
C12048	C12125	C16036	C16232	C17014	C20044	C21045	
C12060	C12141	C16039	C16237	C17015	C20070	C21050	
C12063	C12163	C16047	C16238	C17016	C20079	C21060	
Souther Pacific coastal plain and hills							
C12009	C12025	C12079	C12127	C12232	C12241	C16239	
C12016	C12034	C12086	C12173	C12234	C12244	C20350	
C12017	C12041	C12099	C12188	C12236	C16208	C20378	
C12022	C12069	C12112	C12214	C12240	C16227		
Sierra Madre del Sur							
C12015	C12072	C12106	C12186	C12228	C20076	C20265	C20379
C12028	C12078	C12107	C12195	C12231	C20103	C20271	C20500
C12037	C12083	C12113	C12205	C12248	C20150	C20313	
C12042	C12089	C12140	C12211	C20023	C20153	C20364	
C12054	C12104	C12178	C12227	C20038	C20245	C20367	
Transversal Neovolcanic System							
C12117	C15173	C15256	C15305	C16020	C21031	C21119	C29032
C12128	C15174	C15265	C15328	C16097	C21034	C21129	C29040
C15016	C15184	C15270	C15336	C16098	C21035	C21148	C29041
C15038	C15197	C15272	C15350	C16123	C21038	C21167	C29042
C15039	C15199	C15283	C15353	C16146	C21040	C29002	C29043
C15051	C15205	C15285	C15366	C16235	C21073	C29004	C29047
C15066	C15223	C15287	C15368	C16258	C21077	C29005	C29051
C15088	C15241	C15296	C15371	C16515	C21078	C29007	C29052
C15118	C15248	C15297	C15374	C17019	C21080	C29011	
C15133	C15252	C15298	C15378	C21005	C21081	C29026	
C15134	C15254	C15299	C15391	C21016	C21096	C29027	
C15160	C15255	C15301	C15392	C21026	C21117	C29030	